

On constraining projections of future climate using observations and simulations from multiple climate models

Philip G. Sansom, David B. Stephenson
University of Exeter
and
Thomas J. Bracegirdle
British Antarctic Survey

February 9, 2022

Abstract

Numerical climate models are used to project future climate change due to both anthropogenic and natural causes. Differences between projections from different climate models are a major source of uncertainty about future climate. Emergent relationships shared by multiple climate models have the potential to constrain our uncertainty when combined with historical observations. We combine projections from 13 climate models with observational data to quantify the impact of emergent relationships on projections of future warming in the Arctic at the end of the 21st century. We propose a hierarchical Bayesian framework based on a coexchangeable representation of the relationship between climate models and the Earth system. We show how emergent constraints fit into the coexchangeable representation, and extend it to account for internal variability simulated by the models and natural variability in the Earth system. Our analysis shows that projected warming in some regions of the Arctic may be more than 2 °C lower and our uncertainty reduced by up to 30% when constrained by historical observations. A detailed theoretical comparison with existing multi-model projection frameworks is also provided. In particular, we show that projections may be biased if we do not account for internal variability in climate model predictions.

Keywords: Emergent constraints; Bayesian modeling; Hierarchical models; Measurement error; CMIP5.

1 Introduction

Scientific inquiry into complex systems such as the climate naturally leads to multiple models of a system. The situation in climate science is unusual since different climate models are not treated as incompatible or competing. Instead, each model is treated as a plausible representation of the climate system [Parker, 2006]. This has led to the use of multi-model ensembles to quantify the uncertainty in projections of future climate introduced by choices in model design, usually referred to simply as model uncertainty [Tebaldi and Knutti, 2007]. Statistical methods are required to interpret projections from multi-model ensembles and to make credible probabilistic inferences about future climate change.

In addition to model uncertainty, projections of future climate are subject to a number of other sources of uncertainty. Model inadequacy refers to differences between the models and the Earth system, e.g., missing processes [Craig et al., 2001, Stainforth et al., 2007]. We intuitively think of climate as the distribution of weather. [Stainforth et al., 2007, Stephenson et al., 2012, Rougier and Goldstein, 2014]. Natural variability refers to the range of possible conditions we might experience and is sometimes referred to as sampling uncertainty, since we only observe a single actualization of the Earth system [Chandler, 2013]. Climate models attempt to simulate natural variability by performing multiple simulations from slightly different initial conditions. This is known as internal variability or initial condition uncertainty. Climate projections are also subject to forcing uncertainty and parameter uncertainty. Forcing uncertainty arises due to uncertainty about future emissions of greenhouse gases, both anthropogenic and natural. Parameter uncertainty refers to uncertainty about choice of the internal parameters in climate models [Collins, 2007]. Forcing uncertainty is usually circumvented by making projections rather than predictions of future climate, i.e., predictions conditioned on an assumed future emissions scenario, e.g., Moss et al. [2010]. The computational cost of running sufficiently large perturbed-parameter experiments to span the full range of parameter uncertainty for a single climate model can be prohibitive. Therefore multi-model ensembles usually consist of a set of “best estimates”, i.e., a single version of each model with the internal parameters fixed [Knutti et al., 2010b].

In this paper, we develop a hierarchical Bayesian framework for combining projections from multiple models, applied to projecting climate change in the Arctic at the end of the 21st century. The proposed framework separates model uncertainty and model inadequacy, and accounts for internal variability and natural variability in future projections. In addition, we are able constrain projections of future climate using historical observations (where suitable constraints have been identified) while accounting for uncertainty in the observations.

In order to make projections of future climate from multi-model ensembles, it is necessary to make assumptions about the relationship between climate models and the Earth system. One widely used assumption is that skill in reproducing past climate implies skill in projecting future climate. Climate scientists have long recognized that no single model will perform best for all variables or in all regions [Lambert and Boer, 2001, Jun et al., 2008]. Various approaches have

been proposed for weighting projections from multiple climate models based on their ability to reproduce past climate, these include heuristics [Sanderson et al., 2015b,a, Knutti et al., 2017], multiple regression [Greene et al., 2006, Bishop and Abramowitz, 2013], pattern scaling [Shiogama et al., 2011, Watterson and Whetton, 2011] and Bayesian Model Averaging [Min and Hense, 2006, Bhat et al., 2011]. However, Weigel et al. [2010] demonstrated that weights that do not accurately reflect the projection skill of the models can lead to less reliable projections than weighting all models equally. Long-term climate projection involves extrapolation to states that have not been observed in recent Earth history. Therefore, the ability to reproduce observed data does not guarantee skill for projecting future events [Oreskes et al., 1994]. However, we should certainly be cautious when interpreting projections from models that are not able to adequately reproduce observed data, although how such performance should be quantified remains an open question [Knutti et al., 2010b].

Weighting all models equally implies that each climate model performs equally well for simulating future climate *change*. This has led to the alternative assumption that any bias between the models and the Earth system remains approximately constant over time [Buser et al., 2009]. Under this assumption, two main interpretations of multi-model experiments have emerged [Stephenson et al., 2012]. The “truth plus error” approach treats the output of each model as the “true” state of the Earth system plus some error that is unique to each model [Cubasch et al., 2001, Tebaldi et al., 2005, Furrer et al., 2007b,a, Smith et al., 2009, Tebaldi and Sansó, 2009]. The “exchangeable” approach treats the Earth system as though it were just another climate model, i.e., our inferences about the future climate of the Earth system should be the same as for a climate model with an identical historical climate [Räisänen and Palmer, 2001, Annan and Hargreaves, 2010, 2011]. Neither interpretation is entirely satisfactory. The truth-plus-error interpretation implies that we can improve the precision (but not necessarily the accuracy) of our projections of future climate simply by adding more models to our ensemble. [Annan and Hargreaves, 2010, Knutti et al., 2010a]. The exchangeable interpretation ignores the inherent differences between computer models and the physical systems they seek to represent [Craig et al., 2001, Kennedy and O’Hagan, 2001].

Both the truth-plus error and exchangeable approaches acknowledge differences between models, and between individual models and the Earth system. What is missing are differences from the Earth system that are *common* to all models. All climate models are based on a shared but limited knowledge of the Earth system and face similar technological constraints (e.g., similar numerical methods, available CPU time, memory, etc.), so common limitations will inevitably occur [Stainforth et al., 2007]. To address this issue, Chandler [2013] and Rougier et al. [2013] independently introduced the idea of representing common model errors as a discrepancy between the expected state of the Earth system and a “consensus” or “representative” model. This has the effect of separating model uncertainty (differences between models) from model inadequacy (common differences between models and the Earth system).

Historical observations have been used in a variety of ways to constrain pro-

jections from individual models [Collins et al., 2012]. However, if systematic relationships existed between the historical states and climate responses simulated by *multiple* models, then it might be possible to constrain projections of future climate in a multi-model ensemble without assigning weights to individual models. One of the earliest examples of such a relationship was noted by Allen and Ingram [2002] who referred to it as an “emergent constraint”, since it emerged from analysis of a collection of model simulations rather than by direct calculation based on theory. There is now a growing body of evidence that such relationships may exist at the local or process level, and even at the global level [Hall et al., 2019, Brient, 2020]. In general, we prefer the term “emergent relationship”. We reserve the term “emergent constraint” for when physical insight indicates that the relationship should also hold in the Earth system. Figure 1 shows an example of a well understood emergent constraint on surface temperature in the Arctic due to albedo feedbacks caused by variations in sea-ice coverage simulated by the models [Bracegirdle and Stephenson, 2012]. Other examples of emergent relationships have been found in the cryosphere [Hall and Qu, 2006, Boé et al., 2009], atmospheric chemistry [Eyring et al., 2007, Karpechko et al., 2013], the carbon cycle [Cox et al., 2013, Wenzel et al., 2014] and various other areas of the Earth system. The constraint on Equilibrium Climate Sensitivity proposed by Cox et al. [2018] is a rare example that was derived from theory, then found to be present in a collection of model simulations. Simple linear regression is often used to estimate emergent relationships. However, projection either implicitly treats the Earth system as exchangeable with the models [e.g., Bracegirdle and Stephenson, 2012, 2013], or simply excludes all models that fall outside the plausible range of the observations [e.g., Hall and Qu, 2006, Qu and Hall, 2014].

Multi-model ensembles are sometimes known as “ensembles of opportunity” since models are not systematically selected to span model uncertainty, and cannot be considered a random sample from some larger population [Stephenson et al., 2012]. In particular, several research centers maintain more than one model, and models from different centers often share common components [Knutti et al., 2013]. Similar models are likely to give similar outputs, leading to clustering that could result in biased inferences if not properly accounted for. This is especially important when analyzing emergent constraints since a large cluster of outlying models could strongly influence any regression relationship. Therefore, care is required to ensure that our assumptions in representing model uncertainty and inadequacy are satisfied.

Model uncertainty/inadequacy tends to dominate other sources of uncertainty in long-term climate projections [Hawkins and Sutton, 2009, Yip et al., 2011]. However, there is now a significant body of work highlighting the importance of internal variability and natural variability [Deser et al., 2012, Thompson et al., 2015, McKinnon and Deser, 2018]. Several studies have shown that the contribution of internal variability is non-negligible compared to model uncertainty for some variables at the global scale, and particularly at the regional scale [Hawkins and Sutton, 2009, 2011, Northrop and Chandler, 2014]. The internal variability simulated by each model is indicated by the whiskers in Figure 1.

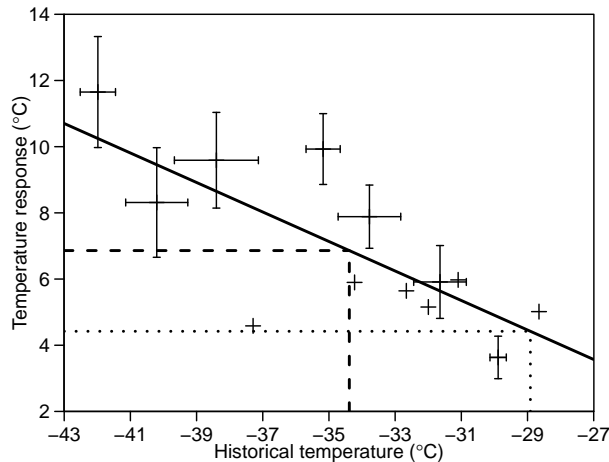


Figure 1: Near-surface warming in the Canadian Arctic Archipelago. Thirty-year mean temperature change between 1975–2005 and 2069–2099 as simulated by an ensemble of 13 climate models under the RCP4.5 mid-range mitigation scenario, for a $2.5^\circ \times 2.5^\circ$ grid box centered on Melville Island ($76^\circ\text{N}, 111^\circ\text{W}$). Crosses mark the mean climate and climate response simulated by each model. Whiskers indicate the range of 30-year mean outcomes from the initial condition runs of each model. The dashed line indicates the mean climate and climate response of the ensemble. The solid line is a simple linear regression estimate of the emergent relationship between the climate response and the historical climate. The dotted line indicates the observed historical climate and projected climate response given the estimated emergent relationship.

Current frameworks for multi-model inference often ignore internal variability and select a single initial condition run from each model [e.g., Tebaldi et al., 2005, Smith et al., 2009, Bishop and Abramowitz, 2013] or take the average over all runs from each model [e.g., Watterson and Whetton, 2011, Bracegirdle and Stephenson, 2012]. Measurement and representation errors in our observations of the climate system can also contribute significant observation uncertainty. Some authors have accounted for observation uncertainty [e.g., Bowman et al., 2018, Cox et al., 2018], but it is frequently ignored and plays an important role if we want to constrain future projections using past observations.

The remainder of this study proceeds as follows. Section 2 outlines the data used to project future warming in the Arctic. In Section 3, we develop a hierarchical Bayesian framework for inferring time mean future climate from multi-model experiments for any future time period and location for which we have model simulations, conditional on simulations of a recent period for which we have corresponding observations. We do not attempt to account for spatial correlation between locations or temporal variation within each time period. Section 4 compares our proposed framework to existing multi-model ensemble

approaches. In Section 5, we apply our framework to the projection of future climate change in the Arctic. We end with concluding remarks in Section 6.

2 Future climate change in the Arctic

The magnitude of the projected warming in the polar regions is much greater than at lower latitudes [Holland and Bitz, 2003]. We use outputs from 13 climate models participating in the World Climate Research Programme’s Coupled Model Intercomparison Project phase 5 [CMIP5, Taylor et al., 2012] to investigate the impact of emergent constraints on projections of winter (December-January-February) near-surface (2 m) temperature change in the Arctic. We compare the 30 year average winter temperature between two time periods. The climate models included and the number of initial condition runs available for each time period are listed in Table 1. The historical period is defined as between December 1975 and January 2005, as simulated under the CMIP5 historical emissions scenario. The future period of interest is between December 2069 and January 2099, as simulated under the RCP4.5 mid-range mitigation scenario [Moss et al., 2010]. The domain of interest is 45°N–90°N, including not only the Arctic Ocean but also the Bering Sea and the Sea of Okhotsk, both of which also currently experience significant seasonal sea ice coverage. Due to the presence of seasonal ice coverage and the complexity associated with modeling it, both model uncertainty and internal variability in near-surface temperature are much greater in the Arctic than at lower latitudes [Northrop and Chandler, 2014]. Prior to analysis, data from all models were interpolated bicubically to a common grid with equal 2.5° spacing in both longitude and latitude.

Observational data in the Arctic are very sparse and no spatially complete data sets exist that include estimates of observational uncertainty. Therefore, we combine four contemporary reanalysis data sets (ERA-Interim [Dee et al., 2011], NCEP CFSR [Saha et al., 2010], JRA-25 [Onogi et al., 2007], NASA MERRA [Rienecker et al., 2011]) using the methodology proposed in Section 3.4. Reanalysis data was interpolated to the same grid as the models.

3 A hierarchical framework for multi-model experiments

The proposed framework is summarized in graphical form in Figure 2. We compare one historical time period denoted H and one future time period denoted F , conditioned on a single future emissions scenario. The top level of Figure 2 consists of quantities for which we have data, i.e., model outputs (X_{Hmr}, X_{Fmr}) and observations (Z_H). The mid-level consists of the climates of the individual models and the Earth system, quantified by the means (X_{Hm}, X_{Fm}, Y_H, Y_F) and variances ($\sigma_m^2, \psi_m^2, \sigma_a^2, \psi_a^2$) of the simulated or plausible conditions during each time period. The bottom level consists of parameters quantifying model uncertainty, the “representative” climate of the ensemble, model inadequacy,

Table 1: Multi-model ensemble. Number of runs available from each model for the historical and future time periods.

Modeling center	Model	Runs	
		Historical	Future
		N_{Hm}	N_{Fm}
BCC	BCC-CSM1.1(m)	3	1
CCCMA	CanESM2	5	5
NSF-DOE-NCAR	CESM1(CAM5)	3	3
ICHEC	EC-EARTH	8	9
LASG-CESS	FGOALS-g2	5	1
NOAA GFDL	GFDL-ESM2G	1	1
NASA GISS	GISS-E2-R	6	6
MOHC	HadGEM2-ES	4	4
INM	INM-CM4	1	1
IPSL	IPSL-CM5A-MR	3	1
MIROC	MIROC5	5	3
MPI-M	MPI-ESM-LR	3	3
MRI	MRI-CGCM3	3	1
Total		50	39

and observation uncertainty. All of these quantities will be fully defined in the development that follows.

We proceed in three stages. First, we propose a hierarchical model for the outputs of the multi-model ensemble (left hand side, Figure 2). Second, we propose a similar hierarchical model for the climate of the Earth system (middle right, Figure 2). Finally, we specify a model for the relationship between the actualized climate and the observations (right hand side, Figure 2).

3.1 The multi-model ensemble

Suppose we have an ensemble of M climate models. Each model performs a number of runs of the historical and future time periods, conditioned on a single future emissions scenario. Each run is initialized from slightly perturbed initial conditions. Let X_{tmr} be the output of run r , during time period $t = \{H, F\}$, by model $m = 1, \dots, M$. The outputs X_{tmr} are assumed to be time averages over periods of equal length. The number of runs of each model for each time period is denoted R_{tm} , i.e., $r = 1, \dots, R_{tm}$ for model m in time period t . We do *not* require that the number of runs from each model be equal, or that the number of runs of each period by a particular model be equal (frequently $R_{Fm} < R_{Hm}$). Each model is attempting to simulate the same target, i.e., the climate of the Earth system under a specific emissions scenario. Therefore, we assume *a priori* that the model outputs X_{tmr} are exchangeable, conditional on the emissions scenario. Exchangeability implies that we hold the same prior beliefs about the output of every run from every model, given a particular scenario. Therefore, we should specify the same probability model for each run of a particular scenario

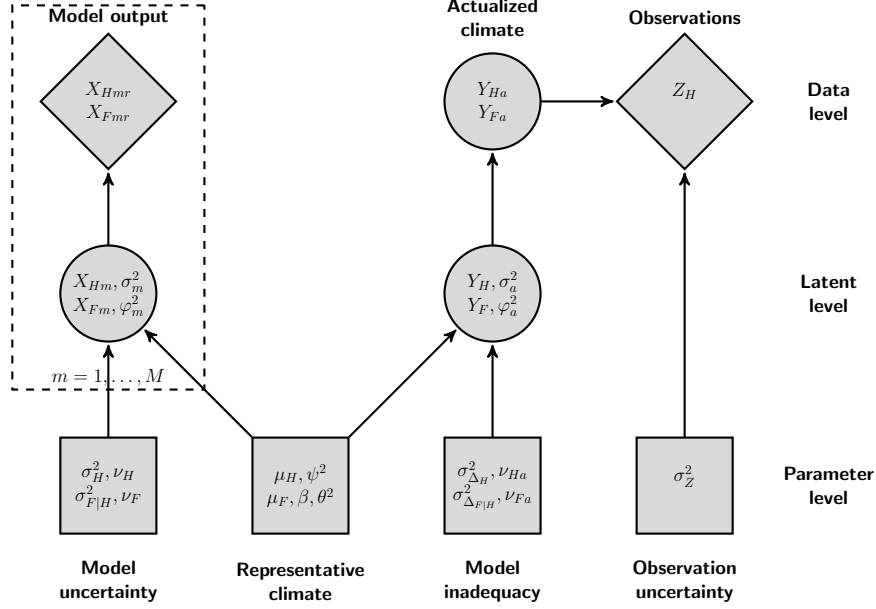


Figure 2: Graphical representation. The proposed framework represented as a directed acyclic graph. Diamonds represent data, circles represent latent quantities, and squares represent parameters. The dashed box represents the multi-model ensemble. The actualized climate Y_{ta} is placed at the data level to emphasize its relationship with the model runs X_{tmr} .

from every model. We model the individual runs X_{tmr} as

$$X_{Hmr} | X_{Hm} \sim N(X_{Hm}, \sigma_m^2) \quad X_{Fmr} | X_{Fm} \sim N(X_{Fm}, (\varphi_m \sigma_m)^2). \quad (1)$$

The outputs X_{tmr} are assumed to be independent between runs r , conditional on the other parameters. The model specific means X_{tm} represent the expected climate of model m at time t . The model specific variances σ_m^2 quantify the spread of the runs from each model in the historical period, i.e., internal variability. The coefficients φ_m^2 allow the internal variability of each model to change in the future period. We assume that the historical and future periods are sufficiently separated in time that departures due to internal variability can be considered independent between periods.

In order to satisfy the assumption of exchangeability between the model outputs, we must also specify the same probability model for the expected climate of each model X_{Hm} and X_{Fm} , and the internal variability of each model σ_m^2 and φ_m^2 . We model the expected climates as

$$X_{Hm} \sim N(\mu_H, \sigma_H^2) \quad X_{Fm} | X_{Hm} \sim N(\mu_F + \beta(X_{Hm} - \mu_H), \sigma_{F|H}^2) \quad (2)$$

and the internal variabilities as

$$\sigma_m^2 \sim \text{Inv-gamma} \left(\frac{\nu_H}{2}, \frac{\nu_H \psi^2}{2} \right) \quad \varphi_m^2 \sim \text{Inv-gamma} \left(\frac{\nu_F}{2}, \frac{\nu_F \theta^2}{2} \right). \quad (3)$$

The model specific parameters X_{Hm} , X_{Fm} , σ_m^2 and φ_m^2 are assumed to be independent between models m , conditional on the other parameters. The common means μ_H and μ_F in Equation 2 are interpreted as the representative climate of the ensemble in the historical and future periods respectively, i.e., representative in the sense that they summarize the climates simulated by the models. The variances σ_H^2 and $\sigma_{F|H}^2$ quantify the spread of the models around the representative climate, i.e., model uncertainty. The parametrization of the internal variabilities in Equation 3 implies that $\psi^2 = 1/\text{E}[\sigma_m^{-2}]$, $\theta^2 = 1/\text{E}[\varphi_m^{-2}]$ and $\theta^2 \psi^2 = 1/\text{E}[(\varphi_m \sigma_m)^{-2}]$. Therefore, ψ^2 and θ^2 can be interpreted as the representative internal variability of the ensemble. The degrees-of-freedom ν_H and ν_F control the precision of σ_m^2 and φ_m^2 and quantify model uncertainty about the internal variability.

The parameter β is intended to capture any linear association between the historical climates and future climate responses of the models, i.e., any emergent relationship, and is referred to as the *emergent constraint*. The emergent constraint applies to the expected climates of the models, not the individual runs, because emergent relationships are the result of model/process differences, not internal variability. A value of $\beta = 1$ implies conditional independence of the expected response $X_{Fm} - X_{Hm}$ of model m from its expected historical state X_{Hm} , i.e., $\text{E}[X_{Fm} - X_{Hm} | X_{Hm}] = \mu_F - \mu_H$ for all m . Any value of $\beta \neq 1$ implies that the expected historical climate X_{Hm} is informative for the expected climate response $X_{Fm} - X_{Hm}$.

The representation in terms of the common unknown means, μ_H and μ_F , induces a common prior correlation (dependence) between the model means and consequently the model outputs, e.g., $\text{cov}(X_{Hm}, X_{Hm'}) = \text{var}(\mu_H)$ for all $m \neq m'$. Thus, we do not require the much stronger assumption that the model outputs are independent.

3.2 The Earth system

Let Y_{ta} represent the single actualization of the Earth system that we observe during time period t . We model the actualized climate as

$$Y_{Ha} | Y_H \sim N(Y_H, \sigma_a^2) \quad Y_{Fa} | Y_F \sim N(Y_F, (\varphi_a \sigma_a)^2). \quad (4)$$

The means Y_H and Y_F represent the expected climate of the Earth system in the historical and future periods respectively. The variance σ_a^2 quantifies the historical natural variability in the Earth system, and the coefficient φ_a^2 represents any future change in variability.

Since each model attempts to approximate the Earth system as realistically as possible, we should hope that the both the expected climate and internal

variability simulated by each model is informative climate of the Earth system. While there are differences between individual climate models, both the mean climates and internal variabilities are usually similar to the Earth system, i.e., the observed quantities usually (but not always) lie within the range simulated by the different models [Flato et al., 2013]. We model the expected climate and natural variability of the Earth system conditional on the representative model as

$$Y_H \sim N(\mu_H, \sigma_{\Delta_H}^2) \quad Y_F | Y_H \sim N(\mu_F + \beta(Y_H - \mu_H), \sigma_{\Delta_{F|H}}^2) \quad (5)$$

and

$$\sigma_a^2 \sim \text{Inv-gamma}\left(\frac{\nu_{Ha}}{2}, \frac{\nu_{Ha}\psi^2}{2}\right) \quad \varphi_a^2 \sim \text{Inv-gamma}\left(\frac{\nu_{Fa}}{2}, \frac{\nu_{Fa}\theta^2}{2}\right). \quad (6)$$

In Equation 5, we assume that the emergent constraint β has a well understood physical basis, and therefore applies to the Earth system in the same way as the climate models. The variances $\sigma_{\Delta_H}^2$ and $\sigma_{\Delta_{F|H}}^2$ quantify our uncertainty about the effects of common differences between the models and the Earth system, i.e., model inadequacy. Equation 6 implies that $E[1/\sigma_a^2] = 1/\psi^2$ and $E[1/\varphi_a^2] = 1/\theta^2$. The degrees-of-freedom ν_{Ha} and ν_{Fa} quantify model inadequacy in simulating natural variability in the Earth system. In the language of Rougier et al. [2013], the Earth system is assumed to be *coexchangeable* with the models. Conditioning on the representative model induces a correlation (dependence) between the expected climate and the model means, i.e., $\text{cov}(Y_H, X_{Hm}) = \text{var}(\mu_H)$ for all m .

3.3 The observed climate

Let Z_H be the observed climate during the historical period. We model the observed climate as

$$Z_H \sim N(Y_{Ha}, \sigma_Z^2). \quad (7)$$

The variance σ_Z^2 quantifies our observation uncertainty.

3.4 Making inferences about future climate

The multi-model ensemble is described by nine parameters μ_H , μ_F , β , σ_H^2 , $\sigma_{F|H}^2$, ψ^2 , θ^2 , ν_H , and ν_F . Given outputs from a moderate number of climate models M , it should be possible to obtain reasonable inferences for the mean parameters μ_H , μ_F and β , and the model uncertainty σ_H^2 and $\sigma_{F|H}^2$. The internal variability ψ^2 and θ^2 can be distinguished from model uncertainty provided we have multiple initial condition runs from several models. Some models may have only a single initial condition run in one or both time periods. In that case, our hierarchical framework allows the model specific internal variability σ_m^2 and φ_m^2 to be estimated by borrowing strength from models with multiple runs, under the assumption that models should have similar internal variability

(Equation 3). The most difficult parameters to infer are likely to be the degrees-of-freedom ν_H and ν_F , since these are essentially variances of variances.

The Earth system is represented by a further four parameters $\sigma_{\Delta_H}^2$, $\sigma_{\Delta_{F|H}}^2$, ν_{Ha} and ν_{Fa} . The future parameters $\sigma_{\Delta_{F|H}}^2$ and ν_{Fa} cannot be estimated from data, since we have no future observations of the Earth system. Therefore, additional modeling assumptions are required. If an estimate of the historical natural variability σ_a^2 is available, then this can be substituted directly, otherwise it can be inferred from the representative model using Equation 6.

3.4.1 Model inadequacy

In principle, the historical model inadequacy quantified by $\sigma_{\Delta_H}^2$ and ν_{Ha} could be estimated from a time series of observations and corresponding simulations. This would require careful modeling to account for time-varying trends and to separate model inadequacy from internal variability and natural variability. In addition, an *extremely* long time series would be required, since the discrepancy between the Earth system and the ensemble is expected to change only slowly over time. Instead, we adopt the approach proposed by Rougier et al. [2013] and parameterize the model inadequacy as proportional to the ensemble spread

$$\begin{aligned} \sigma_{\Delta_H}^2 &= \kappa^2 \sigma_H^2 & \sigma_{\Delta_{F|H}}^2 &= \kappa^2 \sigma_{F|H}^2 \\ \nu_{Ha} &= \nu_H / \kappa^2 & \nu_{Fa} &= \nu_F / \kappa^2 \end{aligned} \quad (8)$$

where $\kappa \geq 1$. The coefficient κ acts to inflate the ensemble spread in order to account for uncertainty due to processes not captured by any model, and errors common to all models. Setting $\kappa = 1$ implies that the Earth system is exchangeable with the climate models, i.e., just another computer model. The value of κ must be fixed *a priori*, and Rougier et al. [2013] suggest a value of $\kappa = 1.2$ for surface temperature. Larger values of κ might be appropriate for less well simulated processes, e.g., when the models are less informative for the real world and the observations lie outside of the spread in the models.

3.4.2 Observation uncertainty

Estimates of the observation uncertainty σ_Z^2 are often not readily available. Several modeling centers produce “reanalysis” products that combine multiple observation sources using complex data assimilation techniques and numerical weather models. Given multiple reanalysis data sets we can approximate our uncertainty about the observed state of the climate. Let W_i be the output of reanalysis i , which we model as

$$W_i \sim N(\mu_W, \sigma_W^2) \quad (9)$$

where μ_W is interpreted as a representative reanalysis and the variance σ_W^2 quantifies the spread of the reanalyses. We expect the representative reanalysis

μ_W to be similar to the actualized climate Y_{Ha} , and so we model the representative reanalysis as

$$\mu_W \sim N(Y_{Ha}, \sigma_{\Delta_W}^2) \quad (10)$$

The variance $\sigma_{\Delta_W}^2$ quantifies our uncertainty about the discrepancy between the representative reanalysis and the actual climate, due to sparsity of observations, errors in the numerical weather models etc. Similar to the models, we judge that the representative reanalysis is less like the actualized climate than the individual reanalyses are like the representative reanalysis, so we set

$$\sigma_{\Delta_W}^2 = \kappa_W^2 \sigma_W^2 \quad \kappa_W \geq 1. \quad (11)$$

Conditioning the representative reanalysis μ_W on the actualized climate Y_{Ha} in Equation 10 induces a correlation (dependence) between the models and the reanalyses, i.e, $\text{cov}(W_i, X_{Hm}) = \text{var}(\mu_H) + \sigma_{\Delta_H}^2 + \sigma_a^2 + \sigma_{\Delta_W}^2$ for all $\{i, m\}$. Such a correlation makes sense, since climate models and reanalyses are very closely related, sharing very similar numerical cores.

4 Discussion and comparison to previous frameworks

The framework proposed in Section 3 was developed to model temperature data for which the normal distribution is a natural choice. However, since the model outputs $X_{t_{mr}}$ are assumed to be time-averages, e.g., 30-year means, the Central Limit Theorem guarantees that the distribution of the $X_{t_{mr}}$ should converge to a normal distribution, regardless of the underlying distribution. Therefore, the proposed framework should be suitable for a wide range of other climate variables. If necessary, different distributional choices can be substituted provided the hierarchical structure is respected in order to maintain the assumption of exchangeability between the model outputs.

In our application, the historical and future variables are the same, i.e., temperature. However, there are many examples of emergent relationships in the literature between different variables in the historical and future periods, e.g., Cox et al. [2018] relate historical temperature variability to Equilibrium Climate Sensitivity. The framework proposed in Section 3 is easily generalized to the case of different historical and future variables by making the future internal variability independent of the historical internal variability in Equation 1, and likewise the natural variability in Equation 4, i.e. $\text{var}(X_{Fmr}) = \varphi_m^2$ rather than $\text{var}(X_{Fmr}) = \varphi_m^2 \sigma_m^2$. No other changes are necessary since all other quantities are specified independently for historical and future variables.

The formulation of the emergent relationship in Equations 2 and 5 reflects the linear relationships that have so far been documented in the literature. Bracegirdle and Stephenson [2012] also considered quadratic relationships and Hall et al. [2019] propose the existence of more general functional relationships.

The methodology proposed here generalizes immediately to polynomial relationships and could easily be generalized to other parametric forms.

In Equations 2 and 3 we assume that the climate models are exchangeable, that is, they can be considered independent conditional on the representative model. If we treat models that share common components as independent then we risk unfairly weighting particular groups of models. Methods for assessing model dependence based on comparing spatial-temporal outputs have been shown to successfully capture similarities between groups of related models [Masson and Knutti, 2011, Knutti et al., 2013]. However, current methods lack a formal statistical framework for combining projections from different models, and can produce unexpected results where models that are known to have little in common are considered close [Sanderson et al., 2015a]. Rougier et al. [2013] address the problem of model dependence by selecting a subset of models that they judge *a priori* to be exchangeable. We adopt a similar approach in Section 5 based on readily available data about climate model structure and components shared between models. By analyzing only a subset of the available data we risk losing valuable information. However, the information loss is likely to be acceptable given the known similarities between many climate models [Annan and Hargreaves, 2011, Pennell and Reichler, 2011]

The framework proposed here makes no assumptions about spatial dependence. Climate model output is often analyzed grid box by grid box, and this is the approach we take in Section 5. In practice, non-physical discontinuities between neighboring grid boxes are rarely a problem due to the inherent smoothness of computer model output in comparison to observations. Accounting for spatial dependence could potentially lead to more efficient estimates by borrowing strength across neighboring grid boxes. However, any increase in efficiency would come at the cost of additional complexity both in terms of the number of parameters and the computational requirements of fitting to all grid boxes simultaneously. Several approaches have been proposed for modeling spatial structure in multi-model ensemble outputs, including harmonic basis functions [Furrer et al., 2007b], kernel mixing [Bhat et al., 2011], and principal components [Rougier et al., 2013, Sanderson et al., 2015a]. However, it is not clear which (if any) of these approaches is most appropriate for multi-model experiments. Differences in feature placement between models can result in overly smooth estimates that do not reflect the physical structure of the underlying field. The methodology proposed here ensures that although posterior mean estimates may be over-smoothed in place, we retain uncertainty due to differences in feature placement thanks to explicit characterization of model uncertainty and inadequacy.

In the framework proposed here, we adopt the approach introduced by Chandler [2013] and Rougier et al. [2013] and represent multi-model inadequacy as an unknown discrepancy between the climate system and a representative model. This generalizes the well established single model approach in the uncertainty quantification literature [Craig et al., 2001, Kennedy and O’Hagan, 2001] by splitting the discrepancy into two parts: one common to all models, and one unique to each model. The limitations of climate models in approximating the

Earth system may manifest themselves in a variety of ways. In the absence of stronger beliefs about how these limitations will manifest, an unknown discrepancy is the simplest and most intuitive way of representing the possibility. Other approaches to representing model inadequacy in an ensemble of computer models may be possible, but we are not aware of any published alternatives.

In the introduction, we made the distinction between a purely statistical “emergent relationship”, and an “emergent constraint” for which a plausible physical mechanism has been identified. Hall et al. [2019] make a similar distinction between what they call “proposed” and “confirmed” emergent constraints, and outline how a constraint might transition from “proposed” to “confirmed”. In formulating our framework, we assume that the emergent constraint applies in the Earth system the same way it does in the models. This assumption is implicit in *all* projections based on emergent constraints, although never stated. By formulating a principled statistical framework, we make this assumption clear and transparent. Thus, by making a projection based on an emergent relationship, we are making a strong statement of confidence in that relationship. The framework proposed here addresses this by separating model inadequacy from model uncertainty, i.e., by allowing for additional uncertainty about the response of the Earth system. However, the appropriate amount of additional uncertainty remains a subjective choice.

4.1 Ensemble regression

Bracegirdle and Stephenson [2012] proposed a method for projection using emergent constraints known as “ensemble regression”. Ensemble regression is equivalent to simple linear regression of the model mean responses on the model mean historical climates, and can be written in our notation as

$$\bar{X}_{Fm} - \bar{X}_{Hm} \sim N\left(\bar{X}_F - \bar{X}_H + \beta'(\bar{X}_{Hm} - \bar{X}_H), \sigma_{F|H}^2\right)$$

where $\bar{X}_{tm} = \sum_r X_{tmr}/R_{tm}$ and $\bar{X}_t = \sum_m \bar{X}_{tm}/M$. This is equivalent to our Equation 2 where $\beta' = \beta - 1$, since $E[\bar{X}_{tm}] = X_{tm}$ and $E[\bar{X}_t] = \mu_t$.

Ensemble regression ignores uncertainty due to internal variability in the model means \bar{X}_{Hm} and the ensemble mean \bar{X}_H . It is well known that errors in the independent variable ($\bar{X}_{Hm} - \bar{X}_H$) in a regression will cause the slope estimate to be biased towards zero, a phenomenon known as *regression dilution* or *regression attenuation* [Frost and Thompson, 2000]. Consider a balanced ensemble ($R_{Hm} = R_{Fm} = R$ for all m) in which all models simulate the same internal variability in each time period, i.e., $\sigma_m^2 = \sigma^2$ and $\varphi_m^2 = 1$ for all m . The expected value of the linear regression estimate of the emergent constraint is

$$E[\hat{\beta}'] = \frac{\text{cov}(\bar{X}_{Fm} - \bar{X}_{Hm}, \bar{X}_{Hm} - \bar{X}_H)}{\text{var}(\bar{X}_{Hm} - \bar{X}_H)} = \frac{\beta' \sigma_H^2 - \sigma^2/R}{\sigma_H^2 + \sigma^2/R}$$

where β' is the “true” value of the emergent constraint. The bias is largest when the internal variability σ^2 is large compared to the model uncertainty σ_H^2 , or

when the number of runs R from each model is small. The framework proposed in Section 3 avoids this bias by explicitly modeling internal variability and its relationship to the expected model climates X_{tm} .

In Bracegirdle and Stephenson [2012], the ensemble regression estimate of the response of the Earth system is

$$Y_F - Y_H \sim N\left(\bar{X}_F - \bar{X}_H + \beta'(Z_H - \bar{X}_H), \sigma_{F|H}^2\right).$$

This is equivalent to assuming the Earth system is exchangeable with the models and ignores the possibility of common differences between the models and the Earth system, as well as the effects of observation uncertainty and natural variability. The framework proposed here explicitly allows for common model inadequacy, observation uncertainty and natural variability.

4.2 A simple hierarchical framework

Bowman et al. [2018] propose a hierarchical framework for emergent constraints without explicit reference to climate models. In our notation, the linear normal-theory version is

$$Y_H \sim N(\mu_H, \sigma_H^2) \quad Y_F | Y_H \sim N\left(\mu_F + \beta(Y_H - \mu_H), \sigma_{F|H}^2\right)$$

and $Z_H | Y_H \sim N(Y_H, \sigma_Z^2)$. In practice, the parameters μ_H , μ_F , β , σ_H and $\sigma_{F|H}$ are estimated from an ensemble of climate models by assuming

$$X_{Hm} \sim N(\mu_H, \sigma_H^2) \quad X_{Fm} | X_{Hm} \sim N\left(\mu_F + \beta(X_{Hm} - \mu_H), \sigma_{F|H}^2\right)$$

for all $m = 1, \dots, M$. This is identical to our Equation 2, so the framework proposed by Bowman et al. [2018] is almost equivalent to Ensemble Regression [Bracegirdle and Stephenson, 2012], but allowing for observation uncertainty. However, the inclusion of the prior on Y_H implies that the posterior expectation of Y_F [Bowman et al., 2018, Eqns 11,13,17] is

$$E[Y_F | Z_H] = \mu_F + \beta \frac{\sigma_Z^{-2}}{\sigma_Z^{-2} + \sigma_H^{-2}} (Z_H - \mu_H).$$

So the expected future climate Y_F experiences a shrinkage towards the representative climate μ_F depending on how informative the observations are compared to the models for the historical climate Y_H , i.e., the ratio of σ_Z^2 to σ_H^2 . No attempt is made to account for model inadequacy, the Earth system is implicitly assumed to be exchangeable with the models. Further, only one run from each model is used, thus ignoring internal variability and leaving the estimated emergent relationship vulnerable to regression dilution.

4.3 The coexchangeable framework

Rougier et al. [2013] propose a model of the joint distribution of the historical and future climate in multi-model experiments known as the coexchangeable framework. In our notation

$$\begin{aligned} \mathbf{X}_m &\sim N(\boldsymbol{\mu}, \boldsymbol{\Sigma}) & m = 1, \dots, M \\ \mathbf{Y} &\sim N(\mathbf{A}\boldsymbol{\mu}, \boldsymbol{\Sigma}_\Delta) & Z_H \sim N(Y_H, \sigma_Z^2) \end{aligned}$$

where $\mathbf{X}_m = (X_{Hm}, X_{Fm})^T$, $\mathbf{Y} = (Y_H, Y_F)^T$, $\boldsymbol{\mu} = (\mu_H, \mu_F)^T$. The matrix \mathbf{A} is assumed known and allows for transformation of variables between model world and the real world (the default choice is $\mathbf{A} = \mathbf{I}$, the identity). The exchangeable framework is a special case of the the coexchangeable framework where $\boldsymbol{\Sigma}_\Delta = \boldsymbol{\Sigma}$ and $\mathbf{A} = \mathbf{I}$. The framework proposed here is an extension of the coexchangeable framework with $\mathbf{A} = \mathbf{I}$ and

$$\boldsymbol{\mu} = \begin{pmatrix} \mu_H \\ \mu_F \end{pmatrix} \quad \boldsymbol{\Sigma} = \begin{pmatrix} \sigma_H^2 & \beta\sigma_H^2 \\ \beta\sigma_H^2 & \beta^2\sigma_H^2 + \sigma_{F|H}^2 \end{pmatrix}.$$

However, the basic coexchangeable framework does not distinguish between model differences and internal variability, and does not account for natural variability in the Earth system. The extended framework proposed here accounts for both of these additional sources of uncertainty.

Rougier et al. [2013] suggest the following parametrization of the model inadequacy

$$\boldsymbol{\Sigma}_\Delta = \kappa^2 \boldsymbol{\Sigma} + \mathbf{D}$$

where \mathbf{D} is a diagonal matrix with $\text{diag}(\mathbf{D}) = (D_H^2, D_F^2)^T$. The variances D_H^2 and D_F^2 are intended to guard against overly precise projections when models are in close agreement. However, this parametrization has unexpected consequences for emergent constraints. Standard results for the multivariate normal distribution show that

$$\mathbb{E}[Y_F | Y_H] = \mu_F + \beta^*(Y_H - \mu_H) \quad \text{where} \quad \beta^* = \frac{\text{cov}(Y_F, Y_H)}{\text{var}(Y_H)} = \frac{\kappa^2 \sigma_H^2}{\kappa^2 \sigma_H^2 + D_H^2} \beta$$

The emergent constraint shrinks towards zero by an amount that depends on D_H^2 . This is difficult to defend given that we have assumed the emergent constraint has a physical basis and should apply to the Earth system. Similar terms D_H^2 and $D_{F|H}^2$ could be added to our Equation 8, but without effecting the emergent constraint, since then $\text{cov}(Y_F, Y_H) = \text{var}(Y_H) = \kappa^2 \sigma_H^2 + D_H^2$ and $\beta^* = \beta$. The difference is due to our formulation in terms of conditional rather than marginal variances. Like $\sigma_{\Delta_H}^2$ and $\sigma_{\Delta_{F|H}}^2$, D_H^2 and $D_{F|H}^2$ are difficult to specify *a priori* without additional data. One possibility might be to consider the spread of a family of closely related models as a lower bound for the model inadequacy.

4.4 The generalized truth-plus-error framework

Chandler [2013] proposed an alternative joint framework for multi-model projection

$$\begin{aligned} \mathbf{X}_{mr} &\sim N(\mathbf{X}_m, \boldsymbol{\Sigma}_m) & r = 1, \dots, N_m \\ \mathbf{X}_m &\sim N(\boldsymbol{\mu}, \boldsymbol{\Lambda}_m) & m = 1, \dots, M \\ \boldsymbol{\mu} &\sim N(\mathbf{Y}, \boldsymbol{\Sigma}_\Delta) & Y_{Ha} \sim N(Y_H, \sigma_a^2) \end{aligned}$$

where $\mathbf{X}_{mr} = (X_{Hmr}, X_{Fmr})^T$, $\mathbf{X}_m = (X_{Hm}, X_{Fm})^T$, $\boldsymbol{\mu} = (\mu_H, \mu_F)^T$, $\mathbf{Y} = (Y_H, Y_F)^T$. The variances $\boldsymbol{\Lambda}_{tm}$ represent the propensity of each simulator to deviate from the ensemble consensus. This provides flexibility to incorporate prior knowledge that certain climate models are more or less similar to each other. Internal variability and model inadequacy are both accounted for. In contrast to Rougier et al. [2013], natural variability is accounted for, but observation uncertainty is ignored.

Chandler [2013] suggests estimating the historical model inadequacy from data as $\sigma_{\Delta_H}^2 = (Y_{Ha} - \mu_H)^2$ then setting

$$\boldsymbol{\Sigma}_\Delta = \begin{pmatrix} \sigma_{\Delta_H}^2 & \sigma_{\Delta_H}^2 \\ \sigma_{\Delta_H}^2 & (1 + \kappa)\sigma_{\Delta_H}^2 \end{pmatrix}$$

for $\kappa > 0$. This parametrization ignores any emergent constraints in the projection of the future climate. In addition, estimating $\sigma_{\Delta_H}^2$ from a single observation Y_{Ha} provides very limited information and makes the analysis vulnerable to outlying or spurious measurements.

The frameworks proposed by Chandler [2013] and Rougier et al. [2013] are conceptually very different and appear incompatible. The most obvious difference is the direction of conditioning between the system \mathbf{Y} and the representative or consensus climate $\boldsymbol{\mu}$. However, Rougier et al. [2013] demonstrated that a simplified form of the generalized truth-plus-error framework can be viewed as a special case of the coexchangeable framework (up to the second moments), for particular choices of $\mathbf{A} \neq \mathbf{I}$ and $\boldsymbol{\Sigma}_\Delta$. It is interesting to note that when all the distributions are normal, identical priors are set for related quantities and $\mathbf{A} = \mathbf{I}$, both frameworks produce identical posterior inferences. This is not the case when the assumption of normality is relaxed, and should not be interpreted as meaning that both formulations are equivalent and can be used interchangeably.

Berliner and Kim [2008] also considered the direction of conditioning between climate models the Earth system and concluded that it should be decided by our ability to formulate the relevant distributions, to interpret them, and to perform the necessary computations. We find it more natural to consider the actual climate as the sum of our knowledge (the representative model) plus what we do *not* understand (model inadequacy), than vice-versa. Hence we adopt a coexchangeable representation for the models. In contrast, we use a truth-plus-error representation for the reanalyses in Equation 10. This feels more natural since the reanalyses are trying to approximate an observable (Y_{Ha}), rather than an abstract quantity (“the climate”) for the models.

4.5 Reliability ensemble averaging

Tebaldi et al. [2005] proposed a probabilistic interpretation of the heuristic “reliability ensemble averaging” framework of Giorgi and Mearns [2003]. The framework belongs to the truth-plus-error family, with some interesting features. Multivariate extensions were proposed by Smith et al. [2009] and Tebaldi and Sansó [2009], and a similar spatial framework was proposed by Furrer et al. [2007b]. The basic framework in our notation is given by

$$\begin{aligned} X_{Hm} &\sim N(Y_H, \lambda_m^2) & X_{Fm} | X_{Hm} &\sim N(Y_F + \beta(X_{Hm} - Y_H), (\theta\lambda_m)^2) \\ Y_{Ha} &\sim N(Y_H, \sigma_a^2). \end{aligned}$$

Similar to Chandler [2013], the model climates X_{tm} are conditioned on the Earth system climate Y_t , and the variances λ_m are interpreted as the propensity of each model to deviate from the system. The coefficient θ allows the propensity of the models to differ from the system to change in the future period. Somewhat confusingly, natural variability in the Earth system is accounted for, but internal variability in the models is ignored. Observation uncertainty and model inadequacy are also both neglected.

The framework proposed by Tebaldi et al. [2005] includes something similar to an emergent constraint. It is instructive to consider this alternative formulation in detail. The expectation of the full conditional posterior distribution of future climate [Tebaldi et al., 2005, Eqn. A9] is

$$\mathbb{E}[Y_F | \dots] = \frac{\sum_m \lambda_m^{-2} X_{Fm}}{\sum_m \lambda_m^{-2}} + \beta \left(Y_H - \frac{\sum_m \lambda_m^{-2} X_{Hm}}{\sum_m \lambda_m^{-2}} \right).$$

This is equivalent to our Equation 5, if $\lambda_m^2 = \sigma_H^2$ for all m , i.e., if all the models are exchangeable. Let $\lambda_m^2 = \sigma_H^2$ and $\theta\lambda_m^2 = \sigma_{F|H}^2$ for all m , then the posterior expectation of Y_H [Tebaldi et al., 2005, Eqn. A8] is

$$\mathbb{E}[Y_H | \dots] = \frac{\sigma_a^{-2} Y_{Ha} + M \left(\sigma_H^{-2} \bar{X}_H + \sigma_{F|H}^{-2} \beta (Y_F - \bar{X}_F + \beta \bar{X}_H) \right)}{\sigma_a^{-2} + M \left(\sigma_H^{-2} + M \sigma_{F|H}^{-2} \beta^2 \right)}$$

In comparison, the posterior expectation of Y_H in our framework is

$$\mathbb{E}[Y_H | \dots] = \frac{\sigma_a^{-2} Y_{Ha} + \sigma_H^{-2} \mu_H + \sigma_{F|H}^{-2} \beta (Y_F - \mu_F + \beta \mu_H)}{\sigma_a^{-2} + \sigma_H^{-2} + \sigma_{F|H}^{-2} \beta^2}$$

assuming $\kappa = 1$, i.e., the models are exchangeable with the Earth system. Both estimates are weighted averages of the model outputs and the actualized climate Y_{Ha} . The two estimates effectively differ only in the weight given to the models. Under the framework proposed by Tebaldi et al. [2005], the models receive M times more weight than under our framework. As a result, the posterior expectation of the expected climate Y_H , and consequently the projected climate Y_F , will lie much closer to the consensus climate, and approach the consensus as the

number of models increases. In fact, the framework proposed by Tebaldi et al. [2005] implies that we can learn the expected climate Y_H and Y_F to any degree of precision we require, simply by adding more climate models [Lopez et al., 2006]. Given the existence of shared errors in all climate models, such an assumption is unsupportable. Tebaldi and Sansó [2009] later proposed the inclusion of a common model bias term to address this issue. However, the common bias was treated as a fixed quantity to be estimated, and does not contribute to our uncertainty about the Earth system in the same way as the model inadequacy terms proposed here and by Rougier et al. [2013] and Chandler [2013].

4.6 Model weighting and Bayesian model averaging

A variety of model weighting schemes have been proposed in the literature (see Section 1 for examples), but all have essentially the same functional form

$$Y_t = \sum_{m=1}^M w_m X_{tm}.$$

The actual climate (or climate response) Y_t is modeled as a weighted combination of the model outputs. Depending on the exact formulation, the weights w_m may be constrained to be positive and sum to one. The weights w_m are estimated by comparing observations of the historical climate Y_H with model simulations X_{Hm} of the same period. The same weights are then applied to future simulations X_{Fm} to obtain projections of the future climate Y_F or climate response $Y_F - Y_H$. Bayesian Model Averaging differs from simple model weighting by dressing each simulation X_{tm} with a kernel, so Y_t becomes a mixture model.

In principle, model weighting will respect emergent relationships. Consider the example of Figure 1. If the models closest to the observations receive the most weight, then the projected climate response will be lower than the ensemble mean estimate. However, unless the models further from the observations receive almost zero weight, the projected response will shrink towards the ensemble mean. The amount of shrinkage will depend on the exact form of the weights. In practice, the weights w_m are usually estimated by comparing model performance at multiple locations, often across the entire study region [e.g., Bhat et al., 2011, Knutti et al., 2017]. If the emergent relationship does not apply across the entire region, or varies within the region, then the weights are unlikely to reflect the relationship and the constraining behavior will be lost.

5 Application to Arctic climate change

The CMIP5 ensemble includes output from more than 40 models submitted by over 20 centers around the world. In order to satisfy the assumption of exchangeability in Section 3, we consider a subset of the models that we judge to be approximately exchangeable. The 13 chosen models and the number of

Table 2: Prior probability distributions.

Description	Parameters	Prior
Representative historical climate	μ_H	$N(0, 10^6)$
Representative future climate	μ_F	$N(\mu_H, 10^6)$
Emergent constraint	β	$N(1, 10^6)$
Representative Internal variability	ψ^2, θ^2	<i>Inv-gamma</i> ($10^{-3}, 10^{-3}$)
Model uncertainty	$\sigma_H^2, \sigma_{F H}^2$	<i>Inv-gamma</i> ($10^{-3}, 10^{-3}$)
Degrees-of-freedom	ν_H, ν_F	<i>Exp</i> ($1/M$)
Reanalysis uncertainty	σ_W^2	<i>Inv-gamma</i> ($10^{-3}, 10^{-3}$)

runs available from the historical and future periods are listed in Table 1. The models included in the thinned ensemble were chosen to have similar horizontal and vertical resolutions, but to minimize common component models according to the detailed information in Table 9.A.1 of Flato et al. [2013]. In particular, only one model was retained from any one modeling center, generally the most recent and feature complete version submitted by each center. Full details of the thinning process are given in the supplementary material. Our approach to ensemble thinning differs from that of Rougier et al. [2013] who chose models judged to be most similar to a familiar model, effectively minimizing the differences between the models. In contrast, by choosing models with the fewest common components, we are effectively maximizing the differences between the models. In doing so, we aim to capture the broadest range of uncertainty due to model differences.

5.1 Prior modeling and posterior computation

Before computing posterior projections of late 21st century warming in the Arctic, we need to specify prior distributions for all unknown parameters. For consistency, we adopt the assessment made by Rougier et al. [2013] and set $\kappa = \kappa_W = 1.2$. Vague conjugate prior probability distributions were specified for the parameters and are listed in Table 2. The resulting full conditional posterior distributions all have standard forms with the exception of the degrees-of-freedom ν_H and ν_F . Therefore, posterior inference can be efficiently accomplished by Gibbs' sampling with Metropolis-Hastings steps for ν_H and ν_F . Full details of the posterior sampling procedure are given in the Supplementary Material.

Posterior analysis was performed for each grid box separately. Identical priors were specified at all grid boxes. Four parallel chains were initialized for each grid box, from over-dispersed starting points. Initially, 20 000 samples were performed by each chain for each grid box. The first 10 000 samples were discarded as burn-in, and Gelman-Rubin diagnostics performed on the remaining 10 000 samples [Gelman and Rubin, 1992]. If any random quantity had a potential scale reduction factor greater than 1.10, then sampling was continued for a further 10 000 samples per chain and diagnostics performed again until satisfactory convergence was indicated. We store every 40th sample from the

last 10 000 samples of each chain, leading to a final sample size of 1000 for each grid box. The Metropolis-within-Gibbs’ sampler was implemented in the R statistical computing language [R Core Team, 2018]. Computation time for four parallel chains of 20 000 samples at a single grid box is around 5.5s on a standard Linux workstation. The samplers for all grid boxes converged successfully. Convergence was achieved after the initial 20 000 samples at 50 % of grid boxes. Less than 2 % of grid boxes required more than 100 000 samples before convergence.

5.2 Model checking

Inspection of the posterior distributions showed that, despite the small ensemble size, the ensemble parameters μ_H , μ_F , β , σ_H^2 , $\sigma_{F|H}^2$ and ψ^2 and θ^2 are all very well constrained by the data. As expected, the degrees-of-freedom ν_H and ν_F were only mildly constrained compared to the exponential prior. The interquartile range (IQR) for the mode of ν_H over the 2880 grid boxes was 5–10, and for ν_F the IQR was 5–8, compared to the mode of zero for the exponential prior. However, both ν_H and ν_F tended to have long tails at individual grid boxes. Due to the extremely small sample size, the reanalysis spread σ_W was relatively poorly constrained compared to the other parameters, but the posterior mean was below 2.0 °C at more than 75 % of grid boxes.

Monte Carlo standard errors were computed for each parameter at each grid box [Flegal et al., 2008, 2017]. The Monte Carlo standard error rarely accounted for more than 4.3 % of the posterior standard error, or exceeded 3.8 % of the absolute posterior mean.

Examination of correlation matrices for the posterior samples revealed that only the means μ_H and μ_F are consistently highly correlated (IQR Cor (μ_H, μ_F) 0.69–0.93), which is to be expected given the relationship in Equation 2. Unsurprisingly, the internal variability ψ^2 and θ^2 are also moderately correlated (IQR -0.44 – -0.37). The only other parameters to have consistently non-zero correlation in the posterior samples were ψ^2 and ν_H (IQR 0.13–0.28), and θ^2 and ν_F (IQR 0.08–0.16). Again, this is not surprising given the close relationship between these parameters in Equation 3, and the small number of initial condition runs available from each model. None of these findings is particularly troubling, and so we conclude that the posterior simulation worked well.

We checked the assumption of exchangeability between models using a leave-one-out cross-validation approach similar to Smith et al. [2009] and Rougier et al. [2013]. Each model in turn is left out of the analysis, and the expected response $X_{Fm}^* - X_{Hm}^*$ of a new model is predicted. The predictions are compared to the model output using a probability integral transform, i.e., by computing the probability that the response under the leave-one-out predicted distribution is less than the mean response of the excluded model. If the models are exchangeable, then the distribution over the models of the transformed projections should be uniform. Kolmogorov-Smirnov tests were used to assess uniformity at each grid box (see Figure 3). A small amount of non-uniformity is expected due to shrinkage of the representative climate towards the observations. In Fig-

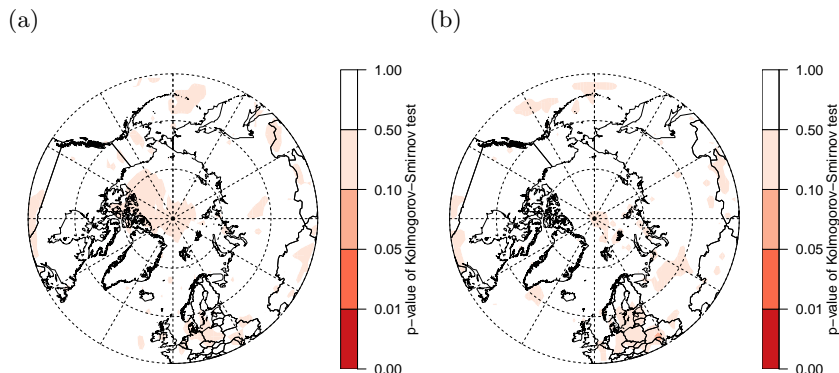


Figure 3: Cross validation. p-values of Kolmogorov-Smirnov tests for uniformity of leave-one-out cross-validated climate response predictions leaving out (a) all data; and (b) only future data from each model in turn.

ure 3a, we withhold all data from each model in turn. There is no evidence against the null hypothesis that the models are exchangeable. No grid boxes are significantly non-uniform at the 10 % level. In Figure 3b, we withhold only the future simulations to test conditional exchangeability given any emergent relationships. Only two grid boxes are significantly non-uniform at the 10 % level. The cross-validation procedure suggests that the chosen models can be considered exchangeable.

5.3 Results

The posterior mean estimates of the expected historical climate Y_H , future climate Y_F , and climate response $Y_F - Y_H$ are shown in Figure 4. The 0°C contour that approximates the sea ice edge has receded noticeably in the projected future climate Y_F in Figure 4b compared to the historical climate Y_H in Figure 4a. The projected warming tends to increase with latitude in Figure 4c.

Figure 5 shows the effects of emergent relationships in near-surface temperature in the Arctic. The posterior mean estimate of the historical discrepancy between the expected climate Y_H and the representative climate μ_H is 2°C – 3°C across most of the Arctic (Figure 5a). The historical discrepancy is largest in the Greenland and Barents seas. This may be due to differences in ocean heat transport simulated by the models [Mahlstein and Knutti, 2011]. From Equation 5, the expected climate response is $E[Y_F - Y_H | Y_H] = \mu_F - \mu_H + (\beta - 1)(Y_H - \mu_H)$. The difference in the projected response due to the emergent relationship is given by $(\beta - 1)(Y_H - \mu_H)$ and is plotted in Figure 5c. The expected warming is reduced by up to 3°C in the far north of Canada, and by around 1°C along most of the ice edge. Figure 5d compares the posterior uncertainty about the climate response $Y_F - Y_H$ with and without an emergent constraint. Around the ice edge, the emergent constraint reduces the posterior standard deviation of the

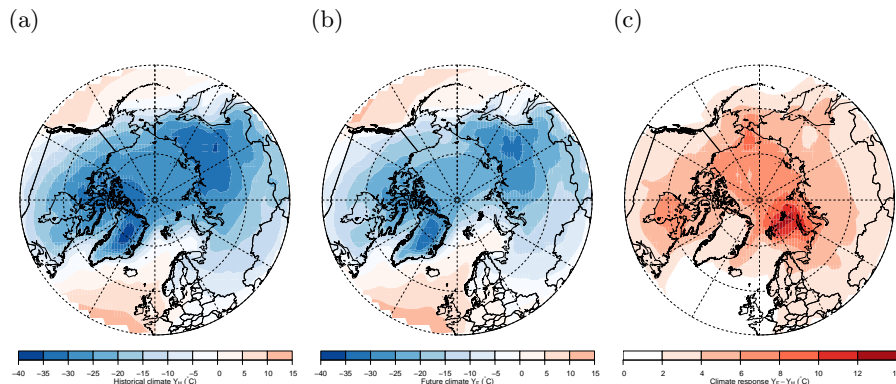


Figure 4: Expected climate. The posterior mean of (a) the historical climate Y_H ; (b) the future climate Y_F ; and (c) the climate response $Y_F - Y_H$.

climate response $Y_F - Y_H$ by 20%–30%.

Our posterior mean estimate of the emergent relationship in the Beaufort sea, north of Alaska in Figure 5b, is much greater than that of Bracegirdle and Stephenson [2013]. Internal variability is small compared to model uncertainty in the Arctic (not shown), so the difference is not due to regression dilution in the ensemble regression estimates. Bracegirdle and Stephenson [2013] analyzed an ensemble of 22 CMIP5 models, some of which were excluded from the ensemble analyzed here. Further investigation revealed that two of the models excluded from our analysis are strongly warm biased in this region, and two are strongly cold biased, but all four simulate similar climate responses. This acts to neutralize the emergent relationship evident in the remaining models (not shown) in the analysis of Bracegirdle and Stephenson [2013].

The greatest warming occurs near the islands of Svalbard and Franz Josef Land in the north of the Barents sea. Figure 6a investigates the strong warming near Svalbard in detail. The representative climate response $\mu_F - \mu_H$ in Figure 6a is already high at 10.5°C (90% equal-tailed credible interval 7.7°C – 13.3°C). The representative response may be influenced by 3 models with unusually large responses. There is a positive emergent relationship $\beta = 1.4$ (0.8,2.0) at this grid box, and a historical discrepancy of $Y_H - \mu_H = 3.0^\circ\text{C}$ (-2.7°C , 8.2°C). The emergent relationship predicts an additional 1.1°C (-1.6°C , 4.8°C) of warming. This is relatively insignificant compared to the uncertainty about the response, even when conditioned on the historical climate. The emergent relationship here does little to constrain our uncertainty about the climate response.

Bracegirdle and Stephenson [2013] also estimated a positive emergent relationship over Svalbard, Franz Josef Land and parts of Siberia, similar to that in Figure 5b. The posterior probability that $\beta > 1$ exceeds 0.90 over Western Siberia. Emergent constraints in air temperatures over polar land regions are particularly relevant for constraining estimates of changes in permafrost, which

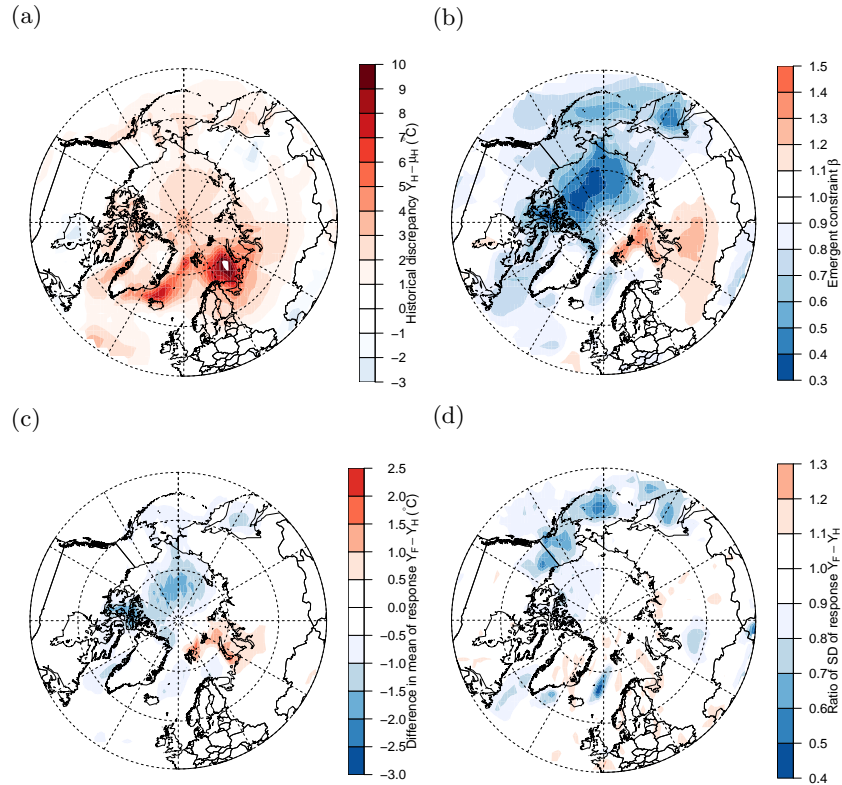


Figure 5: Effect of emergent constraints. The posterior mean of (a) the historical discrepancy $Y_H - \mu_H$, (b) the emergent constraint β , and (c) the difference in the projected climate response Y_H due to the emergent constraint $(\beta - 1)(Y_H - \mu_H)$. (d) Ratio of posterior standard deviation of the response $Y_F - Y_H$ with and without an emergent constraint.

by melting in future could lead to accelerated emissions in greenhouse gases such as methane [Burke et al., 2013]. There are significant differences in model temperatures over polar land regions related to model representation of processes such as snow physics and soil hydrology [Koven et al., 2013, Slater and Lawrence, 2013]. It remains an interesting open question as to why models are showing a positive emergent relationship in the vicinity Western Siberia.

In contrast, a negative emergent relationship is visible in the North West Passage near Devon Island in northern Canada in Figure 6b. The representative climate response $\mu_F - \mu_H$ in Figure 6b is more moderate at 6.6°C ($5.1^\circ\text{C}, 8.0^\circ\text{C}$). There is a negative emergent relationship $\beta = 0.4$ ($0.2, 0.7$) and a historical discrepancy of $Y_H - \mu_H = 3.7^\circ\text{C}$ ($-1.1^\circ\text{C}, 8.4^\circ\text{C}$). The emergent relationship combines with the historical discrepancy to project 2.2°C ($-5.3^\circ\text{C}, 0.6^\circ\text{C}$) less warming than the representative model. At this grid box, our uncertainty is

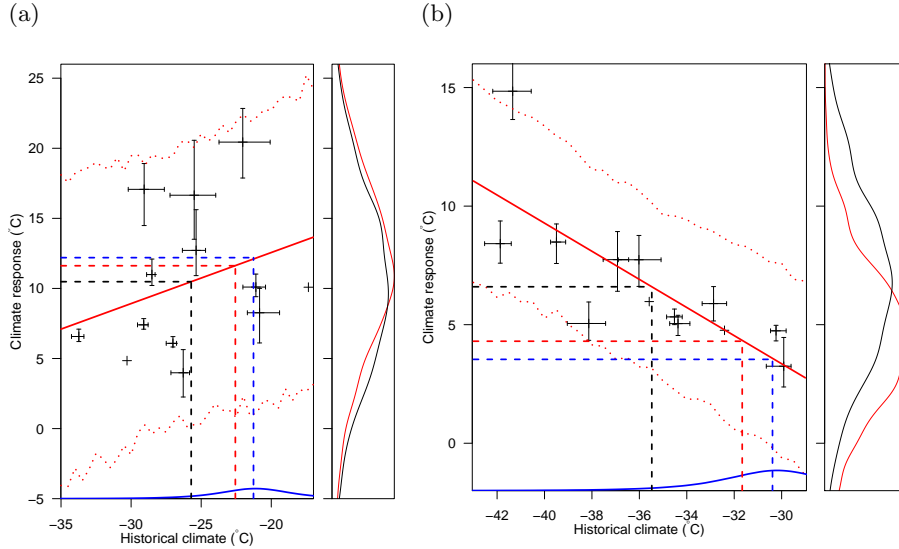


Figure 6: Gridbox details. Data and projections from grid boxes (a) north of Svalbard ($81^{\circ}\text{N}, 39^{\circ}\text{E}$), and (b) east of Devon Island ($76^{\circ}\text{N}, 94^{\circ}\text{W}$). The solid red line indicates the estimated emergent relationship and the dotted red lines indicate a 90% credible interval. The black dashed line indicates the representative climate μ_H and climate response $\mu_F - \mu_H$. The red dashed line indicates the expected climate Y_H and climate response $Y_F - Y_H$. The blue density represents the distribution of the observations. The blue dashed line indicates the observed climate Z_H and the climate response based directly on the observations. Auxiliary plots in the right hand margins show the posterior distribution of the climate response $Y_F - Y_H$ with (red) and without (black) an emergent constraint.

usefully constrained by the emergent relationship. The modification to both the mean and standard deviation of the posterior projected response is shown in the right hand margin of Figure 6b. The posterior standard deviation of the projected response $Y_F - Y_H$ is reduced by 18%, falling from 3.9°C to 3.2°C .

The examples of Svalbard and Devon Island in Figure 6 both demonstrate the important role of observation and sampling uncertainty when combining models and observations. Due to the sparsity of observations in these remote regions, the observation uncertainty is quite large relative to the model uncertainty. In both cases, there is noticeable shrinkage of the posterior mean estimate of the historical climate Y_H away from the observations Z_H and towards the representative climate μ_H . As a result, the projected response $Y_F - Y_H$ lies closer to the representative response $\mu_F - \mu_H$ than it would if observation uncertainty were ignored.

6 Conclusion

Emergent relationships have become an important topic in climate science for their potential to constrain our uncertainty about future climate change. In this study, we have argued that such relationships can be used to constrain discrepancies due to model inadequacy, if a physical mechanism for the relationship can be identified. The negative emergent constraint on near surface temperature in the Arctic is well understood, and our analysis broadly confirms the findings of previous studies. The projected warming in the Arctic is reduced by up to 3 °C by the emergent constraint. Internal variability in the Arctic is large compared to lower latitudes, but is dwarfed by model uncertainty due to the difficulty of representing the many complex processes involved in simulating sea ice, snow cover and the polar vortex. Therefore, regression dilution is unlikely to have significantly biased previous studies of Arctic climate change. However, the sparsity of observations in the Arctic means there is significant observation uncertainty, and this is the first time that observation uncertainty has been accounted for when exploiting emergent constraints. Shrinkage of the expected climate towards the representative climate results in differences of up to 1 °C in the projected response compared to estimates based on the observations directly.

The main contribution of this study is to link the concepts of model inadequacy in an ensemble of models and emergent relationships. The proposed Bayesian hierarchical framework also allows the inclusion of multiple runs from each simulator for the first time in a practical application. This allows us to separate uncertainty due to differences between models from internal variability within models. It is differences in the representation of key processes that lead to emergent relationships. Initial conditions should be forgotten over sufficiently long time scales, and therefore should not lead to emergent behavior. We have shown that if internal variability is not accounted for, then projections based on emergent constraints may be biased. Future multi-model studies exploiting emergent constraints should include multiple runs from each simulator in order to separate model uncertainty from internal variability and avoid potentially biased projections. Another unique aspect of the framework proposed here is the separation of natural variability and observation uncertainty in the climate system.

The framework proposed in this study allows robust estimation and projection using emergent constraints, but there are still open problems to be addressed both in general multi-model experiments and emergent relationships. The methodology proposed here allows projection of time mean climate accounting for uncertainty due to natural variability. If time-series realizations of natural variability are required within the future study period, e.g., for adaptation studies, then our methodology could be extended using the time-series approach proposed by Tebaldi and Sansó [2009], or by transforming observations as proposed by Poppick et al. [2016]. Where emergent constraints have been studied at a local level, rather than an aggregate or process level, they have been analyzed one grid box at a time. Ignoring spatial dependence between grid boxes may lead to overly smooth estimates, due to differences in feature

placement between models. In order to obtain physically realistic inferences, spatial statistical methods are required that can represent spatial dependence while accounting for differences between models.

The CMIP5 multi-model ensemble included four future emissions scenarios, but we have analyzed only one. Like climate models, emissions scenarios are difficult to interpret together as an ensemble. Innovative methods are required to extract meaningful probabilistic projections that span the likely range of future emissions. Another source of uncertainty not usually addressed in multi-model experiments is uncertainty about the internal parameters of the climate models. The computational cost of running large perturbed-parameter ensembles is prohibitive. However, each model undergoes a tuning process during which the internal parameters are tested and fixed [Hourdin et al., 2017]. Statistical emulators for key quantities, trained during this tuning process, might provide a way of integrating parameter uncertainty into multi-model experiments to provide a more holistic assessment of our uncertainty.

In order to satisfy the assumption of exchangeability we analyze only a subset of the available models. By adopting this approach we risk losing valuable information contained in runs from other models and ignoring more detailed insights about model dependence that could be gained by comparing model outputs. In principle, additional levels could be added to the hierarchy proposed here to represent models that share components or were built by the same group. However, the complex overlapping relationships make such a highly structured approach problematic. Current methods for quantifying model dependence based on comparing spatial-temporal output patterns ignore all the prior knowledge we have about the relationships between models. One way forward might be to develop frameworks that combine grouping based on comparing spatial-temporal outputs with simple judgments based on prior knowledge of model inter-dependence. Until alternative methods are found, we recommend thinning the ensemble to obtain an approximately exchangeable set of models and transparently documenting the thinning process. This does require some prior knowledge on the part of the analyst. However, the burden could be alleviated by establishing standard lists of models, e.g., centers submitting to model inter-comparison projects could be asked to nominate a primary model for analysis. This opens up the interesting question of multi-model experiment design. However, the greatest statistical challenge in climate projection is meaningful quantification of model inadequacy. The results here and in Rougier et al. [2013] demonstrate how far we can go with simple judgments. However, additional co-operation between statisticians and climate scientists is required to make further progress.

References

Myles R. Allen and William J. Ingram. Constraints on future changes in climate and the hydrologic cycle. *Nature*, 419(6903):224–232, 2002. doi: 10.1038/nature01092.

- James D. Annan and Julia C. Hargreaves. Reliability of the CMIP3 ensemble. *Geophysical Research Letters*, 37:L02703, 2010. doi: 10.1029/2009GL041994.
- James D. Annan and Julia C. Hargreaves. Understanding the CMIP3 multi-model ensemble. *Journal of Climate*, 24(16):4529–4538, 2011. doi: 10.1175/2011JCLI3873.1.
- L. Mark Berliner and Yongku Kim. Bayesian design and analysis for superensemble-based climate forecasting. *Journal of Climate*, 21(9):1891–1910, 2008. doi: 10.1175/2007JCLI1619.1.
- K. Sham Bhat, Murali Haran, Adam Terando, and Klaus Keller. Climate Projections Using Bayesian Model Averaging and SpaceTime Dependence. *Journal of Agricultural, Biological, and Environmental Statistics*, 16(4):606–628, 2011. doi: 10.1007/s13253-011-0069-3.
- Craig H. Bishop and Gabriel Abramowitz. Climate model dependence and the replicate Earth paradigm. *Climate Dynamics*, 41(3-4):885–900, 2013. doi: 10.1007/s00382-012-1610-y.
- Julien Boé, Alex D. Hall, and Xin Qu. Current GCMs’ Unrealistic Negative Feedback in the Arctic. *Journal of Climate*, 22(17):4682–4695, 2009. doi: 10.1175/2009JCLI2885.1.
- Kevin W. Bowman, Noel Cressie, Xin Qu, and Alex D. Hall. A hierarchical statistical framework for emergent constraints: application to snow-albedo feedback. *Geophysical Research Letters*, 45(23):13050–13059, 2018. doi: 10.1029/2018GL080082.
- Thomas J. Bracegirdle and David B. Stephenson. Higher precision estimates of regional polar warming by ensemble regression of climate model projections. *Climate Dynamics*, 39(12):2805–2821, 2012. doi: 10.1007/s00382-012-1330-3.
- Thomas J. Bracegirdle and David B. Stephenson. On the robustness of emergent constraints used in multimodel climate change projections of arctic warming. *Journal of Climate*, 26(2):669–678, 2013. doi: 10.1175/JCLI-D-12-00537.1.
- Florent Brient. Reducing uncertainties in climate projections with emergent constraints: Concepts, examples and prospects. *Advances in Atmospheric Sciences*, 37:1–15, 2020. doi: 10.1007/s00376-019-9140-8.
- Eleanor J. Burke, Chris D. Jones, and Charles D. Koven. Estimating the permafrost-carbon climate response in the CMIP5 climate models using a simplified approach. *Journal of Climate*, 26(14):4897–4909, 2013. doi: 10.1175/JCLI-D-12-00550.1.
- Christoph M. Buser, Hans R. Künsch, D. Lüthi, M. Wild, and Christoph Schär. Bayesian multi-model projection of climate: Bias assumptions and inter-annual variability. *Climate Dynamics*, 33(6):849–868, 2009. doi: 10.1007/s00382-009-0588-6.

- Richard E. Chandler. Exploiting strength, discounting weakness: combining information from multiple climate simulators. *Philosophical Transactions of the Royal Society A: Mathematical, Physical and Engineering Sciences*, 371: 20120388, 2013. doi: 10.1098/rsta.2012.0388.
- Matthew Collins. Ensembles and probabilities: A new era in the prediction of climate change. *Philosophical Transactions of the Royal Society A: Mathematical, Physical and Engineering Sciences*, 365(1857):1957–1970, 2007. doi: 10.1098/rsta.2007.2068.
- Matthew Collins, Richard E. Chandler, Peter M. Cox, John M. Huthnance, Jonathan Rougier, and David B. Stephenson. Quantifying future climate change. *Nature Climate Change*, 2(6):403–409, 2012. doi: 10.1038/nclimate1414.
- Peter M. Cox, David Pearson, Ben B. Booth, Pierre Friedlingstein, Chris Huntingford, Chris D. Jones, and Catherine M. Luke. Sensitivity of tropical carbon to climate change constrained by carbon dioxide variability. *Nature*, 494(7437):341–4, 2013. doi: 10.1038/nature11882.
- Peter M. Cox, Chris Huntingford, and Mark S. Williamson. Emergent constraint on equilibrium climate sensitivity from global temperature variability. *Nature*, 553(7688):319–322, 2018. doi: 10.1038/nature25450.
- Peter S. Craig, Michael Goldstein, Jonathan C. Rougier, and A. H. Seheult. Bayesian forecasting for complex systems using computer simulations. *Journal of the American Statistical Association*, 96(454):717–729, 2001. doi: 10.1198/016214501753168370.
- U. Cubasch, Gerald A. Meehl, G. J. Boer, Ronald J. Stouffer, M. Dix, A. Noda, Catherine A. Senior, S. Raper, and K. S. Yap. Projections of Future Climate Change. In J.T. Houghton, Y. Ding, D. J. Griggs, M. Noguer, P. J. van der Linden, K. Dai, X. and Maskell, and C. A. Johnson, editors, *Climate Change 2001: The Scientific Bases. Contribution of Working Group I to the Third Assessment Report of the Intergovernmental Panel on Climate Change*, page 881. Cambridge University Press, 2001.
- Dick P. Dee, Sakari M. Uppala, Adrian J. Simmons, Paul Berrisford, Paul Poli, Shinya Kobayashi, U. Andrae, M. A. Balmaseda, G. Balsamo, P. Bauer, P. Bechtold, A. C. M. Beljaars, L. van de Berg, J. Bidlot, N. Bormann, C. Delsol, R. Dragani, M. Fuentes, A. J. Geer, L. Haimberger, S. B. Healy, Hans Hersbach, Elías V. Hólm, Lars Isaksen, Per Kållberg, M. Köhler, M. Matricardi, A. P. McNally, B. M. Monge-Sanz, J. J. Morcrette, B. K. Park, Carole Peubey, P. de Rosnay, C. Tavolato, Jean Noël Thépaut, and Frédéric Vitart. The ERA-Interim reanalysis: Configuration and performance of the data assimilation system. *Quarterly Journal of the Royal Meteorological Society*, 137(656):553–597, 2011. doi: 10.1002/qj.828.

- Clara Deser, Adam S. Phillips, Vincent Bourdette, and Haiyan Teng. Uncertainty in climate change projections: the role of internal variability. *Climate Dynamics*, 38:527–546, 2012. doi: 10.1007/s00382-010-0977-x.
- Veronika Eyring, D. W. Waugh, G. E. Bodeker, E. Cordero, H. Akiyoshi, J. Austin, S. R. Beagley, B. A. Boville, P. Braesicke, C. Brühl, Neal Butchart, M. P. Chipperfield, M. Dameris, R. Deckert, M. Deushi, S. M. Frith, R. R. Garcia, Andrew Gettelman, Marco A. Giorgetta, D. E. Kinnison, E. Mancini, E. Manzini, D. R. Marsh, S. Matthes, T. Nagashima, P. A. Newman, J. E. Nielsen, Steven Pawson, G. Pitari, D. A. Plummer, E. Rozanov, M. Schraner, J. F. Scinocca, K. Semeniuk, T. G. Shepherd, K. Shibata, B. Steil, R. S. Stolarski, W. Tian, and M. Yoshiki. Multimodel projections of stratospheric ozone in the 21st century. *Journal of Geophysical Research: Atmospheres*, 112(D16), 2007. doi: 10.1029/2006JD008332.
- Gregory M. Flato, Jochem Marotzke, Babatunde Abiodun, Pascale Braconnot, Sin Chan Chou, William Collins, Peter M. Cox, Fatima Driouech, Seita Emori, Veronika Eyring, Chris E. Forest, Peter J. Gleckler, Eric Guilyardi, Christian Jakob, Vladimir Kattsov, Chris Reason, and Markku Rummukainen. Evaluation of Climate Models. In Thomas F. Stocker, Dahe Qin, Gian-Kasper Plattner, Melinda M. B. Tignor, Simon K. Allen, Judith Boschung, Alexander Nauels, Yu Xia, Vincent Bex, and Pauline M. Midgley, editors, *Climate Change 2013: The Physical Science Basis. Contribution of Working Group I to the Fifth Assessment Report of the Intergovernmental Panel on Climate Change*. Cambridge University Press, Cambridge, United Kingdom and New York, NY, USA, 2013.
- James M. Flegal, Murali Haran, and Galin L. Jones. Markov Chain Monte Carlo: Can We Trust the Third Significant Figure? *Statistical Science*, 23(2):250–260, 2008. doi: 10.1214/08-STS257.
- James M. Flegal, John Hughes, Dootika Vats, and Ning Dai. mcmcse: Monte Carlo Standard Errors for MCMC, 2017. URL <https://cran.r-project.org/package=mcmcse>.
- Chris Frost and Simon G. Thompson. Correcting for regression dilution bias: comparison of methods for a single predictor variable. *Journal of the Royal Statistical Society: Series A (Statistics in Society)*, 163(2):173–189, 2000. doi: 10.1111/1467-985X.00164.
- Reinhard Furrer, Reto Knutti, Stephan R. Sain, Douglas W. Nychka, and Gerald A. Meehl. Spatial patterns of probabilistic temperature change projections from a multivariate Bayesian analysis. *Geophysical Research Letters*, 34(6):L06711, 2007a. doi: 10.1029/2006GL027754.
- Reinhard Furrer, Stephan R. Sain, Douglas W. Nychka, and Gerald A. Meehl. Multivariate Bayesian analysis of atmosphere-ocean general circulation models. *Environmental and Ecological Statistics*, 14(3):249–266, 2007b. doi: 10.1007/s10651-007-0018-z.

- Andrew Gelman and Donald B. Rubin. Inference from Iterative Simulation Using Multiple Sequences. *Statistical Science*, 7(4):457–511, 1992. doi: 10.1214/ss/1177011136.
- Filippo Giorgi and Linda O. Mearns. Probability of regional climate change based on the Reliability Ensemble Averaging (REA) method. *Geophysical Research Letters*, 30(12):1629, 2003. doi: 10.1029/2003GL017130.
- Arthur M. Greene, Lisa Goddard, and Upmanu Lall. Probabilistic multimodel regional temperature change projections. *Journal of Climate*, 19(17):4326–4343, 2006. doi: 10.1175/JCLI3864.1.
- Alex Hall, Peter Cox, Chris Huntingford, and Stephen Klein. Progressing emergent constraints on future climate change. *Nature Climate Change*, 9(4):269–278, 2019. doi: 10.1038/s41558-019-0436-6.
- Alex D. Hall and Xin Qu. Using the current seasonal cycle to constrain snow albedo feedback in future climate change. *Geophysical Research Letters*, 33(3):1–4, 2006. doi: 10.1029/2005GL025127.
- Ed Hawkins and Rowan T. Sutton. The Potential to Narrow Uncertainty in Regional Climate Predictions. *Bulletin of the American Meteorological Society*, 90:1095–1107, aug 2009. doi: 10.1175/2009BAMS2607.1.
- Ed Hawkins and Rowan T. Sutton. The potential to narrow uncertainty in projections of regional precipitation change. *Climate Dynamics*, 37(1-2):407–418, jul 2011. doi: 10.1007/s00382-010-0810-6.
- M. M. Holland and Cecilia M. Bitz. Polar amplification of climate change in coupled models. *Climate Dynamics*, 21(3-4):221–232, 2003. doi: 10.1007/s00382-003-0332-6.
- Frédéric Hourdin, Thorsten Mauritsen, Andrew Gettelman, Jean Christophe Golaz, Venkatramani Balaji, Qingyun Duan, Doris Folini, Duoying Ji, Daniel Klocke, Yun Qian, Florian Rauser, Catherine Rio, Lorenzo Tomassini, Masahiro Watanabe, and Daniel Williamson. The art and science of climate model tuning. *Bulletin of the American Meteorological Society*, 98:589–602, 2017. ISSN 00030007. doi: 10.1175/BAMS-D-15-00135.1.
- Mikyoung Jun, Reto Knutti, and Douglas W. Nychka. Spatial Analysis to Quantify Numerical Model Bias and Dependence. *Journal of the American Statistical Association*, 103(483):934–947, 2008. doi: 10.1198/016214507000001265.
- Alexey Yu Karpechko, Douglas Maraun, and Veronika Eyring. Improving Antarctic Total Ozone Projections by a Process-Oriented Multiple Diagnostic Ensemble Regression. *Journal of the Atmospheric Sciences*, 70(12):3959–3976, 2013. doi: 10.1175/JAS-D-13-071.1.

- Marc C Kennedy and Anthony O’Hagan. Bayesian Calibration of Computer Models. *Journal of the Royal Statistical Society: Series B (Statistical Methodology)*, 63(3):425–464, 2001. doi: 10.1111/1467-9868.00294.
- Reto Knutti, Gabriel Abramowitz, Matthew Collins, Veronika Eyring, Peter J. Gleckler, Bruce Hewitson, and Linda O. Mearns. Good Practice Guidance Paper on Assessing and Combining Multi Model Climate Projections. In Thomas Stocker, Qin Dahe, Gian-Kasper Plattner, Melinda Tignor, and Pauline Midgley, editors, *Meeting report of the Intergovernmental Panel On Climate Change Expert Meeting on Assessing and Combining Multiple Model Climate Projections*. {IPCC} Working Group {I} Technical Support Unit, 2010a.
- Reto Knutti, Reinhard Furrer, Claudia Tebaldi, Jan Cermak, and Gerald A. Meehl. Challenges in combining projections from multiple climate models. *Journal of Climate*, 23(10):2739–2758, 2010b. doi: 10.1175/2009JCLI3361.1.
- Reto Knutti, David Masson, and Andrew Gettelman. Climate model genealogy: Generation CMIP5 and how we got there. *Geophysical Research Letters*, 40(6):1194–1199, 2013. doi: 10.1002/grl.50256.
- Reto Knutti, Jan Sedláček, Benjamin M. Sanderson, Ruth Lorenz, Erich M. Fischer, and Veronika Eyring. A climate model projection weighting scheme accounting for performance and interdependence. *Geophysical Research Letters*, 44(4):1909–1918, 2017. doi: 10.1002/2016GL072012.
- Charles D. Koven, William J. Riley, and Alex Stern. Analysis of Permafrost Thermal Dynamics and Response to Climate Change in the CMIP5 Earth System Models. *Journal of Climate*, 26(6):1877–1900, 2013. doi: 10.1175/JCLI-D-12-00228.1.
- S. J. Lambert and G. J. Boer. CMIP1 evaluation and intercomparison of coupled climate models. *Climate Dynamics*, 17(2-3):83–106, 2001. doi: 10.1007/PL00013736.
- Ana Lopez, Claudia Tebaldi, Mark New, David A. Stainforth, Myles R. Allen, and J. A. Kettleborough. Two approaches to quantifying uncertainty in global temperature changes. *Journal of Climate*, 19(19):4785–4796, 2006. doi: 10.1175/JCLI3895.1.
- Irina Mahlstein and Reto Knutti. Ocean heat transport as a cause for model uncertainty in projected arctic warming. *Journal of Climate*, 24(5):1451–1460, 2011. doi: 10.1175/2010JCLI3713.1.
- David Masson and Reto Knutti. Climate model genealogy. *Geophysical Research Letters*, 38(8):L08703, 2011. doi: 10.1029/2011GL046864.
- Karen A. McKinnon and Clara Deser. Internal Variability and Regional Climate Trends in an Observational Large Ensemble. *Journal of Climate*, 31(17):6783–6802, 2018. doi: 10.1175/JCLI-D-17-0901.1.

- Seung Ki Min and Andreas Hense. A Bayesian approach to climate model evaluation and multi-model averaging with an application to global mean surface temperatures from IPCC AR4 coupled climate models. *Geophysical Research Letters*, 33(8):L08708, 2006. doi: 10.1029/2006GL025779.
- Richard H. Moss, Jae A. Edmonds, Kathy A. Hibbard, Martin R. Manning, Steven K. Rose, Detlef P. van Vuuren, Timothy R. Carter, Seita Emori, Mikiko Kainuma, Tom Kram, Gerald A. Meehl, John F. B. Mitchell, Nebojsa Nakicenovic, Keywan Riahi, Steven J. Smith, Ronald J. Stouffer, Allison M. Thomson, John P. Weyant, and Thomas J. Wilbanks. The next generation of scenarios for climate change research and assessment. *Nature*, 463(7282):747–756, 2010. doi: 10.1038/nature08823.
- Paul J. Northrop and Richard E. Chandler. Quantifying Sources of Uncertainty in Projections of Future Climate. *Journal of Climate*, 27(23):8793–8808, 2014. doi: 10.1175/JCLI-D-14-00265.1.
- Kazutoshi Onogi, Junichi Tsutsui, Hiroshi Koide, Masami Sakamoto, Shinya Kobayashi, Hiroaki Hatsushika, Takanori Matsumoto, Nobuo Yamazaki, Hirohisa Kamahori, Kiyotoshi Takahashi, Shinji Kadokura, Koji Wada, Koji Kato, Ryo Oyama, Tomoaki Ose, Nobutaka Mannoji, and Ryusuke Taira. The JRA-25 Reanalysis. *Journal of the Meteorological Society of Japan*, 85(3):369–432, 2007. doi: 10.2151/jmsj.85.369.
- Naomi Oreskes, Kristin Shrader-Frechette, and Kenneth Belitz. Verification, Validation, and Confirmation of Numerical Models in the Earth Sciences. *Science*, 263(5147):641–646, 1994. doi: 10.1126/science.263.5147.641.
- W. S. Parker. Understanding pluralism in climate modeling. *Foundations of Science*, 11(4):349–368, 2006. doi: 10.1007/s10699-005-3196-x.
- Christopher Pennell and Thomas Reichler. On the Effective Number of Climate Models. *Journal of Climate*, 24(9):2358–2367, 2011. doi: 10.1175/2010JCLI3814.1.
- Andrew Poppick, David J. McInerney, Elisabeth J. Moyer, and Michael L. Stein. Temperatures in transient climates: Improved methods for simulations with evolving temporal covariances. *The Annals of Applied Statistics*, 10(1):477–505, 2016. doi: 10.1214/16-AOAS903.
- Xin Qu and Alex D. Hall. On the persistent spread in snow-albedo feedback. *Climate Dynamics*, 42(1-2):69–81, 2014. doi: 10.1007/s00382-013-1774-0.
- R Core Team. R: A Language and Environment for Statistical Computing, 2018. URL <https://www.r-project.org>.
- Jouni Räisänen and Timothy N. Palmer. A probability and decision-model analysis of a multimodel ensemble of climate change simulations. *Journal of Climate*, 14(15):3212–3226, 2001. doi: 10.1175/1520-0442(2001)014<3212:APADMA>2.0.CO;2.

- Michele M. Rienecker, Max J. Suarez, Ronald Gelaro, Ricardo Todling, Julio Bacmeister, Emily Liu, Michael G. Bosilovich, Siegfried D. Schubert, Lawrence Takacs, Gi Kong Kim, Stephen Bloom, Junye Chen, Douglas Collins, Austin Conaty, Arlindo Da Silva, Wei Gu, Joanna Joiner, Randal D. Koster, Robert Lucchesi, Andrea Molod, Tommy Owens, Steven Pawson, Philip Pegion, Christopher R. Redder, Rolf Reichle, Franklin R. Robertson, Albert G. Ruddick, Meta Sienkiewicz, and Jack Woollen. MERRA: NASA's modern-era retrospective analysis for research and applications. *Journal of Climate*, 24(14):3624–3648, 2011. doi: 10.1175/JCLI-D-11-00015.1.
- Jonathan C. Rougier and Michael Goldstein. Climate Simulators and Climate Projections. *Annual Review of Statistics and Its Application*, 1(1):103–123, 2014. doi: 10.1146/annurev-statistics-022513-115652.
- Jonathan C. Rougier, Michael Goldstein, and Leanna House. Second-Order Exchangeability Analysis for Multimodel Ensembles. *Journal of the American Statistical Association*, 108(503):852–863, 2013. doi: 10.1080/01621459.2013.802963.
- Suranjana Saha, Shrinivas Moorthi, Hua Lu Pan, Xingren Wu, Jiande Wang, Sudhir Nadiga, Patrick Tripp, Robert Kistler, John Woollen, David Behringer, Haixia Liu, Diane Stokes, Robert Grumbine, George Gayno, Jun Wang, Yu Tai Hou, Hui Ya Chuang, Hann Ming H Juang, Joe Sela, Mark Iredell, Russ Treadon, Daryl Kleist, Paul van Delst, Dennis Keyser, John Derber, Michael Ek, Jesse Meng, Helin Wei, Rongqian Yang, Stephen Lord, Huug van den Dool, Arun Kumar, Wanqiu Wang, Craig Long, Muthuvel Chelliah, Yan Xue, Boyin Huang, Jae Kyung Schemm, Wesley Ebisuzaki, Roger Lin, Pingping Xie, Mingyue Chen, Shuntai Zhou, Wayne Higgins, Cheng Zhi Zou, Quanhua Liu, Yong Chen, Yong Han, Lidia Cucurull, Richard W. Reynolds, Glenn Rutledge, and Mitch Goldberg. The NCEP climate forecast system reanalysis. *Bulletin of the American Meteorological Society*, 91(8):1015–1057, 2010. doi: 10.1175/2010BAMS3001.1.
- Benjamin M. Sanderson, Reto Knutti, and Peter M. Caldwell. Addressing interdependency in a multimodel ensemble by interpolation of model properties. *Journal of Climate*, 28(13):5150–5170, 2015a. doi: 10.1175/JCLI-D-14-00361.1.
- Benjamin M. Sanderson, Reto Knutti, and Peter M. Caldwell. A representative democracy to reduce interdependency in a multimodel ensemble. *Journal of Climate*, 28(13):5171–5194, 2015b. doi: 10.1175/JCLI-D-14-00362.1.
- Hideo Shiogama, Seita Emori, Naota Hanasaki, Manabu Abe, Yuji Masutomi, Kiyoshi Takahashi, and Toru Nozawa. Observational constraints indicate risk of drying in the Amazon basin. *Nature communications*, 2:253, 2011. doi: 10.1038/ncomms1252.

- Andrew G. Slater and David M. Lawrence. Diagnosing present and future permafrost from climate models. *Journal of Climate*, 26(15):5608–5623, 2013. doi: 10.1175/JCLI-D-12-00341.1.
- Richard L. Smith, Claudia Tebaldi, Douglas W. Nychka, and Linda O. Mearns. Bayesian Modeling of Uncertainty in Ensembles of Climate Models. *Journal of the American Statistical Association*, 104(485):97–116, 2009. doi: 10.1198/jasa.2009.0007.
- David A. Stainforth, Myles R. Allen, E. R. Tredger, and Leonard A. Smith. Confidence, uncertainty and decision-support relevance in climate predictions. *Philosophical Transactions of the Royal Society A*, 365:2145–2161, 2007. doi: 10.1098/rsta.2007.2074.
- David B. Stephenson, Matthew Collins, Jonathan C. Rougier, and Richard E. Chandler. Statistical problems in the probabilistic prediction of climate change. *Environmetrics*, 23(5):364–372, 2012. doi: 10.1002/env.2153.
- Karl E. Taylor, Ronald J. Stouffer, and Gerald A. Meehl. An overview of CMIP5 and the experiment design. *Bulletin of the American Meteorological Society*, 93(4):485–498, 2012. doi: 10.1175/BAMS-D-11-00094.1.
- Claudia Tebaldi and Reto Knutti. The use of the multi-model ensemble in probabilistic climate projections. *Philosophical Transactions of the Royal Society A: Mathematical, Physical and Engineering Sciences*, 365(1857):2053–2075, 2007. doi: 10.1098/rsta.2007.2076.
- Claudia Tebaldi and Bruno Sansó. Joint projections of temperature and precipitation change from multiple climate models: A hierarchical Bayesian approach. *Journal of the Royal Statistical Society: Series A (Statistics in Society)*, 172(1):83–106, 2009. doi: 10.1111/j.1467-985X.2008.00545.x.
- Claudia Tebaldi, Richard L. Smith, Douglas W. Nychka, and Linda O. Mearns. Quantifying uncertainty in projections of regional climate change: A Bayesian approach to the analysis of multimodel ensembles. *Journal of Climate*, 18(10):1524–1540, 2005. doi: 10.1175/JCLI3363.1.
- David W. J. Thompson, Elizabeth A. Barnes, Clara Deser, William E. Foust, and Adam S. Phillips. Quantifying the role of internal climate variability in future climate trends. *Journal of Climate*, 28(16):6443–6456, 2015. doi: 10.1175/JCLI-D-14-00830.1.
- I. G. Watterson and P. H. Whetton. Distributions of decadal means of temperature and precipitation change under global warming. *Journal of Geophysical Research: Atmospheres*, 116(7):1–13, 2011. doi: 10.1029/2010JD014502.
- Andreas P. Weigel, Reto Knutti, Mark A. Liniger, and Christof Appenzeller. Risks of model weighting in multimodel climate projections. *Journal of Climate*, 23(15):4175–4191, 2010. doi: 10.1175/2010JCLI3594.1.

Sabrina Wenzel, Peter M. Cox, Veronika Eyring, and Pierre Friedlingstein. Emergent constraints on climate-carbon cycle feedbacks in the CMIP5 Earth system models. *Journal of Geophysical Research: Biogeosciences*, 119(5):794–807, 2014. doi: 10.1002/2013JG002591.

Stan Yip, Christopher A. T. Ferro, and David B. Stephenson. A Simple, Coherent Framework for Partitioning Uncertainty in Climate Predictions. *Journal of Climate*, 24(17):4634–4643, 2011. doi: 10.1175/2011JCLI4085.1.

SUPPLEMENTARY MATERIAL

Derivation of Gibbs'-Metropolis updating equations

For the purposes of computation it is more convenient to work with precisions than variances, so let

$$\begin{aligned} \tau_m &= 1/\sigma_m^2 \text{ for } m = 1, \dots, M; & \phi_m &= 1/\varphi_m^2 \text{ for } m = 1, \dots, M \\ \tau_H &= 1/\sigma_H^2; & \tau_{F|H} &= 1/\sigma_{F|H}^2; & \tau_a &= 1/\sigma_a^2; & \phi_a &= 1/\varphi_a^2 \\ \tau_{\Delta_H} &= 1/\sigma_{\Delta_H}^2; & \tau_{\Delta_F} &= 1/\sigma_{\Delta_F}^2; & \tau_W &= 1/\sigma_W^2; & \tau_{\Delta_W} &= 1/\sigma_{\Delta_W}^2. \end{aligned}$$

The complete model defined by Equations 1–8 and 9–11 can be rewritten as

$$\begin{aligned} X_{Hmr} | X_{Hm} &\sim N(X_{Hm}, \tau_m^{-1}) & X_{Fmr} | X_{Fm} &\sim N(X_{Fm}, (\phi_m \tau_m)^{-1}) \\ X_{Hm} &\sim N(\mu_H, \tau_H^{-1}) & X_{Fm} | X_{Hm} &\sim N(\mu_F + \beta(X_{Hm} - \mu_H), \tau_{F|H}^{-1}) \\ \tau_m &\sim Ga\left(\frac{\nu_H}{2}, \frac{\nu_H \psi^2}{2}\right) & \phi_m &\sim Ga\left(\frac{\nu_F}{2}, \frac{\nu_F \theta^2}{2}\right) \\ Y_{Ha} | Y_H &\sim N(Y_H, \tau_a^{-1}) & Y_{Fa} | Y_F &\sim N(Y_F, (\phi_a \tau_a)^{-1}) \\ Y_H &\sim N(\mu_H, \tau_{\Delta_H}^{-1}) & Y_F | Y_H &\sim N(\mu_F + \beta(Y_H - \mu_H), \tau_{\Delta_F}^{-1}) \\ \tau_a &\sim Ga\left(\frac{\nu_{Ha}}{2}, \frac{\nu_{Ha} \psi^2}{2}\right) & \phi_a &\sim Ga\left(\frac{\nu_{Fa}}{2}, \frac{\nu_{Fa} \theta^2}{2}\right) \\ W_i &\sim N(\mu_W, \tau_W^{-1}) & \mu_W &\sim N(Y_{Ha}, \tau_{\Delta_W}^{-1}) \end{aligned}$$

where

$$\begin{aligned} \tau_{\Delta_H} &= \tau_H / \kappa^2 & \tau_{\Delta_{F|H}} &= \tau_{F|H} / \kappa^2 & \tau_{\Delta_W} &= \tau_W / \kappa_W^2 \\ \nu_{Ha} &= \nu_H / \kappa^2 & \nu_{Fa} &= \nu_F / \kappa^2. \end{aligned}$$

Let $\mathbf{X} = (X_{tmr}, s \in \{H, F\}, m = 1, \dots, M, r = 1, \dots, R_{tm})'$ be the model outputs, $\mathbf{Y} = (Y_H, Y_{Ha}, \tau_a)'$ be the latent state of the climate system, $\boldsymbol{\theta} = (\mu_H, \mu_F, \beta, \tau_H, \tau_{F|H}, \psi^2, \phi^2, \nu_H, \nu_F)'$ be the ensemble parameters, $\boldsymbol{\chi} = (X_{Hm}, X_{Fm}, \tau_m, \phi_m, m = 1, \dots, M)'$ be the latent model states, $\mathbf{W} = (W_i, i = 1, \dots, N)$ be the reanalysis outputs, and $\boldsymbol{\omega} = (\mu_W, \tau_W)'$ be the reanalysis parameters. The future state of the climate system defined by Y_F, Y_{Fa} and ϕ_a are purely predictive quantities and can be sampled after sampling of all other quantities is complete, using the equations above.

The joint posterior can be decomposed as

$$\Pr(\mathbf{Y}, \boldsymbol{\chi}, \boldsymbol{\theta}, \boldsymbol{\omega} | \mathbf{X}, \mathbf{W}) \propto \Pr(\mathbf{W} | \boldsymbol{\omega}) \Pr(\mathbf{Y} | \boldsymbol{\theta}, \boldsymbol{\omega}) \Pr(\mathbf{X} | \boldsymbol{\chi}) \Pr(\boldsymbol{\chi} | \boldsymbol{\theta}) \Pr(\boldsymbol{\theta}) \Pr(\boldsymbol{\omega})$$

The likelihood of the reanalysis outputs \mathbf{W} given the reanalysis parameters $\boldsymbol{\omega}$ is proportional to

$$\Pr(\mathbf{W} | \boldsymbol{\omega}) \propto \prod_{i=1}^N \tau_W^{1/2} \exp\left(-\frac{\tau_W}{2} (W_i - \mu_W)^2\right).$$

The likelihood of the system \mathbf{Y} given the ensemble parameters $\boldsymbol{\theta}$ and the reanalysis parameters $\boldsymbol{\omega}$ is proportional to

$$\begin{aligned} \Pr(\mathbf{Y} | \boldsymbol{\theta}, \boldsymbol{\omega}) &\propto \tau_{\Delta_H}^{1/2} \exp\left(-\frac{\tau_{\Delta_H}}{2} (Y_H - \mu_H)^2\right) \tau_a^{1/2} \exp\left(-\frac{\tau_a}{2} (Y_{Ha} - Y_H)^2\right) \\ &\quad \frac{\left(\frac{\nu_{Ha}\psi^2}{2}\right)^{\nu_{Ha}/2}}{\Gamma(\nu_{Ha}/2)} \tau_a^{\nu_{Ha}/2-1} \exp\left(-\frac{\nu_{Ha}\psi^2}{2} \tau_a\right). \end{aligned}$$

The likelihood of the model outputs \mathbf{X} given the latent model states $\boldsymbol{\chi}$ is proportional to

$$\begin{aligned} \Pr(\mathbf{X} | \boldsymbol{\chi}) &\propto \prod_{m=1}^M \prod_{r=1}^{R_{Hm}} \tau_m^{1/2} \exp\left(-\frac{\tau_m}{2} (X_{Hmr} - X_{Hm})^2\right) \\ &\quad \prod_{m=1}^M \prod_{r=1}^{R_{Fm}} (\phi_m \tau_m)^{1/2} \exp\left(-\frac{\phi_m \tau_m}{2} (X_{Fmr} - X_{Fm})^2\right). \end{aligned}$$

The likelihood of the model states $\boldsymbol{\chi}$ given the ensemble parameters $\boldsymbol{\theta}$ is proportional to

$$\begin{aligned} \Pr(\boldsymbol{\chi} | \boldsymbol{\theta}) &\propto \prod_{m=1}^M \tau_H^{1/2} \exp\left(-\frac{\tau_H}{2} (X_{Hm} - \mu_H)^2\right) \\ &\quad \prod_{m=1}^M \tau_F^{1/2} \exp\left(-\frac{\tau_F}{2} (X_{Fm} - \mu_F - \beta (X_{Hm} - \mu_H))^2\right) \\ &\quad \prod_{m=1}^M \frac{\left(\frac{\nu_H\psi^2}{2}\right)^{\nu_H/2}}{\Gamma(\nu_H/2)} \tau_m^{\nu_H/2-1} \exp\left(-\frac{\nu_H\psi^2}{2} \tau_m\right) \\ &\quad \prod_{m=1}^M \frac{\left(\frac{\nu_F\theta^2}{2}\right)^{\nu_F/2}}{\Gamma(\nu_F/2)} \phi_m^{\nu_F/2-1} \exp\left(-\frac{\nu_F\theta^2}{2} \phi_m\right). \end{aligned}$$

The joint prior distribution of the ensemble parameters $\boldsymbol{\theta}$ is proportional to

$$\begin{aligned} \Pr(\boldsymbol{\theta}) &\propto \exp\left(-\frac{b_{\mu_H}}{2} (\mu_H - a_{\mu_H})^2\right) \exp\left(-\frac{b_{\mu_F}}{2} (\mu_F - \mu_H)^2\right) \exp\left(-\frac{b_{\beta}}{2} (\beta - a_{\beta})^2\right) \\ &\quad \tau_H^{a_{\tau_H}-1} \exp(-b_{\tau_H} \tau_H) \tau_F^{a_{\tau_F}-1} \exp(-b_{\tau_F} \tau_F) \nu_H^{a_{\nu_H}-1} \exp(-b_{\nu_H} \nu_H) \nu_F^{a_{\nu_F}-1} \exp(-b_{\nu_F} \nu_F) \\ &\quad (\psi^2)^{a_{\psi^2}-1} \exp(-b_{\psi^2} \psi^2) (\theta^2)^{a_{\theta^2}-1} \exp(-b_{\theta^2} \theta^2). \end{aligned}$$

The joint prior distribution of the reanalysis parameters $\boldsymbol{\omega}$ is proportional to

$$\Pr(\boldsymbol{\omega}) \propto \tau_{\Delta W}^{1/2} \exp\left(-\frac{\tau_{\Delta W}}{2} (\mu_W - Y_{Ha})^2\right) \tau_W^{a\tau_W - 1} \exp(-b\tau_W \tau_W).$$

The full conditional distributions of the system quantities \mathbf{Y} are

$$\begin{aligned} Y_{Ha} | \dots &\sim N\left(\frac{\tau_a Y_H + \tau_{\Delta W} \mu_W}{\tau_a + \tau_{\Delta W}}, (\tau_a + \tau_{\Delta W})^{-1}\right) \\ Y_H | \dots &\sim N\left(\frac{\tau_{\Delta H} \mu_H + \tau_a Y_{Ha}}{\tau_{\Delta H} + \tau_a}, (\tau_{\Delta H} + \tau_a)^{-1}\right) \\ \tau_a | \dots &\sim Ga\left(\frac{\nu_{Ha} + 1}{2}, \frac{\nu_{Ha} \psi^2 + (Y_{Ha} - Y_H)^2}{2}\right) \end{aligned}$$

The full conditional distributions of the reanalysis parameters $\boldsymbol{\omega}$ are

$$\begin{aligned} \mu_W | \dots &\sim N\left(\frac{\tau_W \sum_i W_i + \tau_{\Delta W} Y_{Ha}}{\tau_W N + \tau_{\Delta W}}, (\tau_W N + \tau_{\Delta W})^{-1}\right) \\ \tau_W | \dots &\sim Ga\left(a_{\tau_W} + \frac{N+1}{2}, b_{\tau_W} + \frac{1}{2} \sum_i (W_i - \mu_W)^2 + \frac{1}{2} \kappa_W^{-2} (\mu_W - Y_{Ha})^2\right) \end{aligned}$$

The full conditional distributions of the latent model states $\boldsymbol{\chi}$ are

$$\begin{aligned} X_{Fm} | \dots &\sim N\left(\frac{\tau_F (\mu_F + \beta (X_{Hm} - \mu_H)) + \phi_m \tau_m \sum_r X_{Fmr}}{\tau_F + \phi_m \tau_m R_{Fm}}, (\tau_F + \phi_m \tau_m R_{Fm})^{-1}\right) \\ X_{Hm} | \dots &\sim N\left(\frac{\tau_H \mu_H + \tau_F \beta (X_{Fm} - \mu_F + \beta \mu_H) + \tau_m \sum_r X_{Hmr}}{\tau_H + \tau_F \beta^2 + \tau_m R_{Hm}}, (\tau_H + \tau_F \beta^2 + \tau_m R_{Hm})^{-1}\right) \\ \tau_m | \dots &\sim Ga\left(\frac{\nu_H + N_{Hm} + N_{Fm}}{2}, \frac{\nu_H \psi^2 + \sum_r (X_{Hmr} - X_{Hm})^2 + \phi_m \sum_r (X_{Fmr} - X_{Fm})^2}{2}\right) \\ \phi_m | \dots &\sim Ga\left(\frac{\nu_F + N_{Fm}}{2}, \frac{\nu_F \theta^2 + \tau_m \sum_r (X_{Fmr} - X_{Fm})^2}{2}\right) \end{aligned}$$

The full conditional distributions of the ensemble parameters θ are

$$\begin{aligned}
\mu_H | \dots &\sim N\left(\tilde{\mu}_H, (b_{\mu_H} + b_{\mu_F} + \tau_H M + \tau_F \beta^2 M + \tau_{\Delta_H})^{-1}\right) \\
\mu_F | \dots &\sim N\left(\frac{b_{\mu_F} \mu_H + \tau_F \sum_m (X_{Fm} - \beta(X_{Hm} - \mu_H))}{b_{\mu_F} + \tau_F M}, (b_{\mu_F} + \tau_F M)^{-1}\right) \\
\beta | \dots &\sim N\left(\frac{b_\beta a_\beta + \tau_F \sum_m (X_{Hm} - \mu_H)(X_{Fm} - \mu_F)}{b_\beta + \tau_F \sum_m (X_{Hm} - \mu_H)^2}, \left(b_\beta + \tau_F \sum_m (X_{Hm} - \mu_H)^2\right)^{-1}\right) \\
\tau_H | \dots &\sim Ga\left(a_{\tau_H} + \frac{M+1}{2}, b_{\tau_H} + \frac{\sum_m (X_{Hm} - \mu_H)^2 + \kappa^{-2} (Y_H - \mu_H)^2}{2}\right) \\
\tau_F | \dots &\sim Ga\left(a_{\tau_F} + \frac{M}{2}, b_{\tau_F} + \frac{\sum_m (X_{Fm} - \mu_F - \beta(X_{Hm} - \mu_H))^2}{2}\right) \\
\psi^2 | \dots &\sim Ga\left(a_{\psi^2} + \frac{\nu_H M + \nu_{H_a}}{2}, b_{\psi^2} + \frac{\nu_H \sum_m \tau_m + \nu_{H_a} \tau_a}{2}\right) \\
\theta^2 | \dots &\sim Ga\left(a_{\theta^2} + \frac{\nu_F M}{2}, b_{\theta^2} + \frac{\nu_F \sum_m \phi_m}{2}\right)
\end{aligned}$$

where

$$\tilde{\mu}_H = \frac{b_{\mu_H} a_{\mu_H} + b_{\mu_F} \mu_F + \tau_H \sum_m X_{Hm} - \tau_F \beta \sum_m (X_{Fm} - \mu_F - \beta X_{Hm}) + \tau_{\Delta_H} Y_H}{b_{\mu_H} + b_{\mu_F} + \tau_H M + \tau_F \beta^2 M + \tau_{\Delta_H}}.$$

The full conditional distributions of the degrees-of-freedom ν_H and ν_F do not correspond to any standard distribution. The likelihoods associated with ν_H and ν_F are

$$l(\nu_H) = \frac{\beta_{Ha}^{\alpha_{Ha}}}{\Gamma(\alpha_{Ha})} \tau_a^{\alpha_{Ha}-1} \exp(-\beta_{Ha}\tau_a) \prod_m \frac{\beta_H^{\alpha_H}}{\Gamma(\alpha_H)} \tau_m^{\alpha_H-1} \exp(-\beta_H\tau_m)$$

and

$$l(\nu_F) = \prod_m \frac{\beta_F^{\alpha_F}}{\Gamma(\alpha_F)} \phi_m^{\alpha_F-1} \exp(-\beta_F\phi_m)$$

where

$$\alpha_{Ha} = \nu_{Ha}/2, \quad \beta_{Ha} = \nu_{Ha}\psi^2/2, \quad \alpha_H = \nu_H/2, \quad \beta_H = \nu_H\psi^2/2, \quad \alpha_F = \nu_F/2, \quad \beta_F = \nu_F\theta^2/2.$$

The prior densities of ν_H and ν_F are

$$p(\nu_H) \propto \nu_H^{a\nu_H-1} \exp(-b\nu_H\nu_H) \quad \text{and} \quad p(\nu_F) \propto \nu_F^{a\nu_F-1} \exp(-b\nu_F\nu_F).$$

The posterior distributions of ν_H and ν_F conditional on the current state of the other parameters can be sampled using the Metropolis-Hastings algorithm. For each $s \in \{H, F\}$:

1. Sample a new state ν_t^* from $q(\nu_t^* | \nu_t)$;
2. Calculate the Hastings ratio

$$r(\nu_t^*, \nu_t) = \frac{l(\nu_t^*)p(\nu_t^*)q(\nu_t | \nu_t^*)}{l(\nu_t)p(\nu_t)q(\nu_t^* | \nu_t)};$$

3. Accept the new state ν_t^* with probability

$$a(\nu_t^*, \nu_t) = \min(1, r(\nu_t^*, \nu_t)).$$

where $q(\nu_t^* | \nu_t) = Ga(\nu_t\lambda_t, \lambda_t)$ is the proposal distribution, with expectation ν_t and variance controlled by the free parameter λ_t . The acceptance rate of the Metropolis step can be controlled using the parameter λ_t .

Ensemble thinning

An extended version of the CMIP5 surface temperature data analyzed by Bracegirdle and Stephenson [2013] was considered for analysis. The mean climates over 30 winters (December-January-February) are compared between December 1975 and January 2005 from the historical scenario, and between December 2069 and January 2099 from the RCP4.5 scenario. The five year shift in the historical period compared to Bracegirdle and Stephenson [2013] provides slightly better compatibility with the latest observation and reanalysis data sets. Several of these data sets begin in 1979 when satellite observations become prevalent. A total of 216 runs from 37 CMIP5 models were included in the full ensemble, 128 runs of the historical scenario and 88 of the RCP4.5 scenario. The complete list of models and details of their major components are given in Table 1.

In the main text we noted that not all of the models should be included in the analysis in order to satisfy the assumption of exchangeability. In particular, models from the same center are likely to be more similar than those from different centers. Therefore, only one model from each center should be included. Modeling centers may also share components with other groups. Therefore, where possible only one model using any given major component, or at least any combination of components, should be included.

The full ensemble was thinned in order to satisfy the judgment of exchangeability between the model outputs. The ACCESS models supersede the CSIRO-Mk3.6.0 model, however all of the major components in the ACCESS models are borrowed from other models. Therefore, none of the models submitted by CSIRO were included. Two models were submitted by BCC, the model with the higher resolution atmosphere components was retained. Three models were submitted from the combined efforts of the NSF-DOE-NCAR. The CESM1(CAM5) variant was selected as it includes a more recent version of the CAM atmosphere model. The NCAR CCSM4 model has been superseded by the CESM1 model, and so was not included. The two NorESM1 models are also very closely related to the CESM1 model, so was excluded. The BNU-ESM and FIO-ESM models were also excluded since they use outdated and low resolution versions of the CAM atmosphere included in the CESM1 model. The two models submitted from the CMCC are both based on an old atmosphere component and a very old ocean component. They also lack a full land surface model, therefore neither model was included. The CNRM-CM5 model and EC-EARTH models are very closely related, but EC-EARTH model includes more RCP4.5 runs so was retained over CNRM-CM5. The models from NOAA-GFDL differ primarily in their ocean component. GFDL-ESM2G uses the GOLD ocean model, while GFDL-ESM2M and GFDL-CM3 use the MOM4.1 ocean model. However, the MOM4 ocean model is also used in the models from the BCC, so GFDL-ESM2M and GFDL-CM3 are excluded. The NASA GISS-E2-R model was retained over the GISS-E2-H for the increased number of levels in the ocean model. The MOHC model in its HadGEM2-CC configuration has a relatively low resolution ocean component compared to most of the other models, so it is excluded in favor of the HadGEM2-ES configuration. The model submitted by NIMR/KMA

Modelling centre	Model	Atmosphere	Atmosphere res.	Ocean	Ocean res.	Sea ice	Land surface
CSIRO-BOM	ACCESS1.0	HadGEM2 (r1.1)	1.9 x 1.9 L38	MOM4.1	1.0 x 1.0 L50	CICE4.1	MOSES2.2
CSIRO-BOM	ACCESS1.3	UKMO GA 1.0	1.9 x 1.9 L38	MOM4.1	1.0 x 1.0 L50	CICE4.1	CABLE
BCC	BCC-AGCM2.1	BCC-AGCM2.1	2.8 x 2.8 L26	MOM4-L40	1.0 x 1.0 L40	GFDL SIS	BCC-AVIM1.0
BCC	BCC-CSM1.1(m)	BCC-AGCM2.1	1.1 x 1.1 L26	MOM4-L40	1.0 x 1.0 L40	GFDL SIS	BCC-AVIM1.0
GCESS	BNU-ESM	CAM3.5	2.8 x 2.8 L26	MOM4.1	1.0 x 1.0 L50	CICE4.1	CoLM+BNUDGVM
CCCMA	CanESM2	CanAM4	2.8 x 2.8 L35	CanOM4	1.4 x 1.4 L40	Included	CLASS 2.7; CTEM
NCAR	CCSM4	CAM4	1.2 x 1.2 L27	POP2	1.0 x 1.0 L60	CICE4	CLM4
NSF-DOE-NCAR	CESM1(BGC)	CAM4	1.2 x 1.2 L27	POP2	1.0 x 1.0 L60	CICE4	CLM4
NSF-DOE-NCAR	CESM1(CAM5)	CAM5	1.2 x 1.2 L27	POP2	1.0 x 1.0 L60	CICE4	CLM4
NSF-DOE-NCAR	CESM1(WACCM)	WACCM4	2.5 x 2.5 L66	POP2	1.0 x 1.0 L60	CICE4	CLM4
CMCC	CMCC-CM	ECHAM5	0.8 x 0.8 L31	OPAS.2	2.0 x 2.0 L31	LIM2	N / A
CMCC	CMCC-CMS	ECHAM5	1.9 x 1.9 L95	OPAS.2	2.0 x 2.0 L31	LIM2	N / A
CNRM-CERFACS	CNRM-CM5	ARPEGE-Climate	1.4 x 1.4 L31	NEMO	0.7 x 0.7 L42	Gelato5	SURFEX
CSIRO-QCCCE	CSIRO-Mk3.6.0	Included	1.9 x 1.9 L18	MOM2.2	1.9 x 1.9 L31	Included	Included
EC-EARTH	EC-EARTH	IFS c3 1r1	1.1 x 1.1 L62	NEMO_ecmwf	1.0 x 1.0 L31	LIM2	HTESSEL
LASG-CES	FGOALS-g2	CAM3.0	2.8 x 2.8 L26	LICOM2	1.0 x 1.0 L30	CICE4-LASG	CLM3
FIO	FIO-ESM	CAM3.0	2.8 x 2.8 L26	POP2	1.0 x 1.0 L40	CICE4	CLM3.5
NOAA GFDL	GFDL-CM3	Included	2.5 x 2.5 L48	MOM4.1	1.0 x 1.0 L50	SIS	Included
NOAA GFDL	GFDL-ESM2G	AM2.1	2.5 x 2.5 L24	GOLD	1.0 x 1.0 L63	SIS	Included
NOAA GFDL	GFDL-ESM2M	AM2.1	2.5 x 2.5 L60	MOM4.1	1.0 x 1.0 L50	SIS	Included
NASA GISS	GISS-E2-H	Included	2.5 x 2.5 L40	HYCOM	1.0 x 1.0 L26	SIS	Included
NASA GISS	GISS-E2-R	Included	2.5 x 2.5 L40	Russell	1.0 x 1.0 L32	Included	Included
NIMR/KMA	HadGEM2-AO	HadGAM2	1.9 x 1.9 L60	Included	1.9 x 1.9	Included	Included
MOHC	HadGEM2-CC	HadGAM2	1.9 x 1.9 L60	Included	1.9 x 1.9	Included	Included
MOHC	HadGEM2-ES	HadGAM2	1.9 x 1.9 L38	Included	1.0 x 1.0 L40	Included	Included
INM	INM-CM4	Included	2.0 x 2.0 L21	Included	1.0 x 1.0 L40	Included	Included
IPSL	IPSL-CM5A-LR	LMDZ5	3.8 x 3.8 L39	NEMO	2.0 x 2.0 L31	Included	Included
IPSL	IPSL-CM5A-MR	LMDZ5	2.5 x 2.5 L39	NEMO	2.0 x 2.0 L31	Included	Included
IPSL	IPSL-CM5B-LR	LMDZ5	3.8 x 3.8 L39	NEMO	2.0 x 2.0 L31	Included	Included
MIROC	MIROC5	MIROC-AGCM6	1.4 x 1.4 L40	COCOA.5	1.4 x 1.4 L50	Included	MATSIRO
MIROC	MIROC-ESM	MIROC-AGCM	2.8 x 2.8 L80	COCOA.4	1.4 x 1.4 L44	Included	MATSIRO
MIROC	MIROC-ESM-CHEM	MIROC-AGCM	2.8 x 2.8 L80	COCOA.4	1.4 x 1.4 L44	Included	MATSIRO
MPI-M	MPI-ESM-LR	ECHAM6	1.9 x 1.9 L47	MPTOM	1.5 x 1.5 L40	Included	JSBACH
MPI-M	MPI-ESM-MR	ECHAM6	1.9 x 1.9 L95	MPTOM	0.4 x 0.4 L40	Included	JSBACH
MRI	MRI-CGCM3	MRI-AGCM3.3	1.1 x 1.1 L48	MRI-COM3	1.0 x 1.0 L50	MRI-COM3	HAL
NCC	NorESM1-M	CAM4-Oslo	2.5 x 2.5 L26	NorESM-Ocean	1.1 x 1.1 L53	CICE4	CLM4
NCC	NorESM1-ME	CAM4-Oslo	2.5 x 2.5 L26	NorESM-Ocean	1.1 x 1.1 L53	CICE4	CLM4

Table 1: Structural details of the 37 CMIP5 models included in the analysis of Arctic surface temperature. Models highlighted in red are included in the exchangeable ensemble. Atmosphere and ocean resolution are in degrees and Lxx indicates the number of vertical levels. Details included in this table were gathered from the metadata included in the model outputs and supplemented using information from Table 9.A.1 of Flato et al. [2013].

is another version of the MOHC model, and so was excluded. The resolution of the atmospheric component of the IPSL-CM5A-LR model is also low compared to the rest of the ensemble, so it is excluded in favor of the IPSL-CM5A-MR configuration. Similarly, the atmospheric resolution of the MIROC models in their MIROC-ESM configuration is relatively low, so they are excluded and MIROC5 is retained. In contrast, the MPI-ESM-MR configuration features a very high resolution ocean component compared to the rest of the ensemble. Therefore the MPI-ESM-LR configuration is retained instead. This leaves an ensemble of 89 runs from 13 models, 50 runs from the historical scenario and 39 from the RCP4.5 scenario.

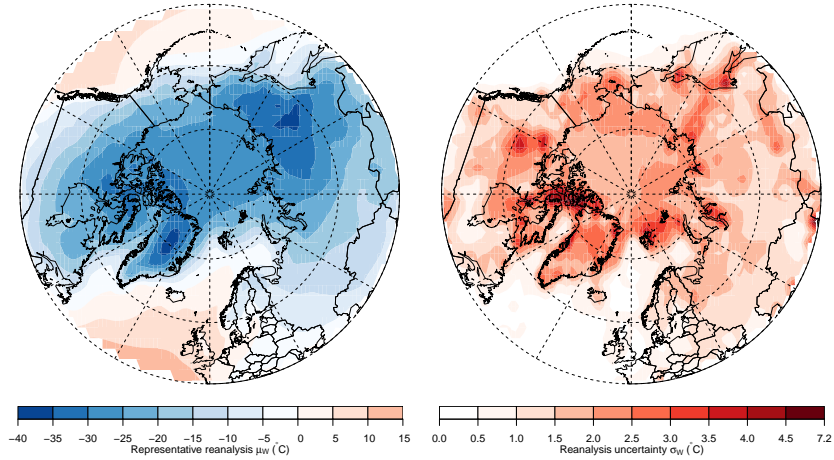


Figure 1: Posterior mean estimates of the representative reanalysis μ_W and the reanalysis uncertainty σ_W .

Posterior parameter estimates

The spread between the reanalyses σ_W is greater over land than over the ocean where temperatures vary more slowly (Figure 1). The reanalysis uncertainty increases with latitude as the number of observing stations decreases and the terrain tends to become more mountainous (Figure 1). The spread between the reanalyses is particularly large around the sea ice edge.

The representative historical climate μ_H is quite similar to the representative reanalysis μ_W , except over the Arctic ocean where climate models tend to be cold biased (Figure 2). The historical spread between the models σ_H is generally greater than the spread between the reanalyses σ_W (Figure 2). Like the reanalyses, the model spread tends to be greatest over mountainous regions and near the sea ice edge.

The model response uncertainty $\sigma_{F|H}$ is greatest over the Arctic ocean, particularly to the east of Svalbard (Figure 3).

Like the reanalysis uncertainty, the representative internal variability ψ is greater over land than over the oceans, and highest in mountainous regions and close to the sea ice edge (Figure 4). The representative change in internal variability θ is small over most of the study area (Figure 4). Internal variability decreases close to the historical sea ice edge, where rising temperatures cause the ice edge to retreat and temperatures to stabilize. The climate in the interior of the Arctic becomes more variable as rising temperatures causes seasonal melting in regions permanently covered by sea ice during the historical period.

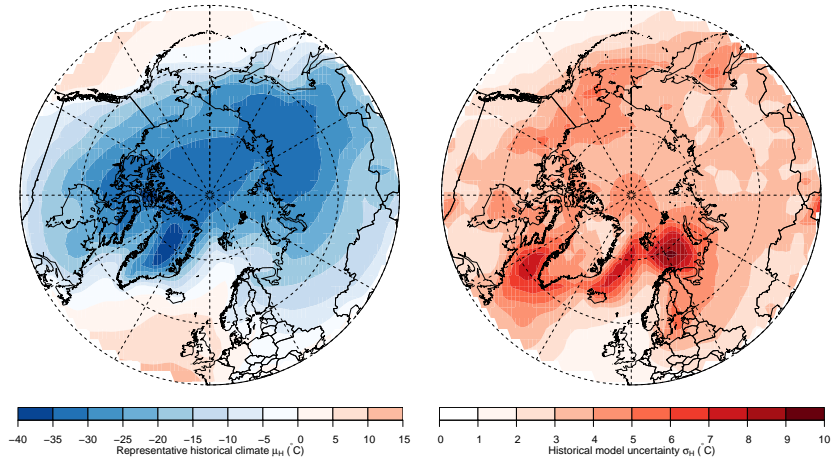


Figure 2: Posterior mean estimates of the representative historical climate μ_H and the historical model uncertainty σ_H .

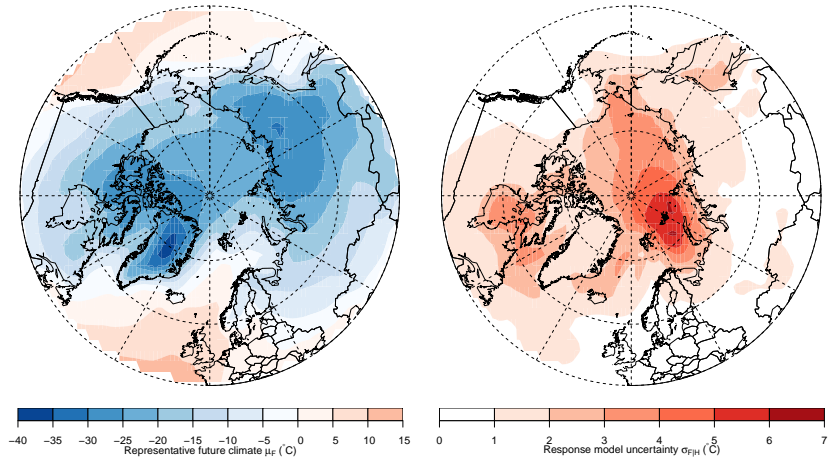


Figure 3: Posterior mean estimates of the representative future climate μ_F and the model response uncertainty $\sigma_{F|H}$.

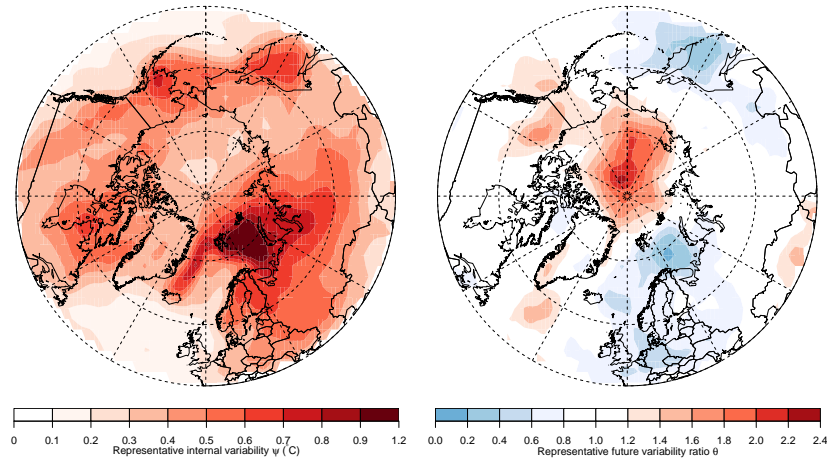


Figure 4: Posterior mean estimates of the representative historical internal variability ψ and change in internal variability θ .

References

- Thomas J. Bracegirdle and David B. Stephenson. On the robustness of emergent constraints used in multimodel climate change projections of arctic warming. *Journal of Climate*, 26(2):669–678, 2013. doi: 10.1175/JCLI-D-12-00537.1.
- Gregory M. Flato, Jochem Marotzke, Babatunde Abiodun, Pascale Braconnot, Sin Chan Chou, William Collins, Peter M. Cox, Fatima Driouech, Seita Emori, Veronika Eyring, Chris E. Forest, Peter J. Gleckler, Eric Guilyardi, Christian Jakob, Vladimir Kattsov, Chris Reason, and Markku Rummukainen. Evaluation of Climate Models. In Thomas F. Stocker, Dahe Qin, Gian-Kasper Plattner, Melinda M. B. Tignor, Simon K. Allen, Judith Boschung, Alexander Nauels, Yu Xia, Vincent Bex, and Pauline M. Midgley, editors, *Climate Change 2013: The Physical Science Basis. Contribution of Working Group I to the Fifth Assessment Report of the Intergovernmental Panel on Climate Change*. Cambridge University Press, Cambridge, United Kingdom and New York, NY, USA, 2013.